Cell. Mol. Life Sci. 66 (2009) 275 – 300

Review

The continuing disappearance of "pure" Ca^{2+} buffers

B. Schwaller

Unit of Anatomy, Department of Medicine, University of Fribourg, Route Albert-Gockel 1, 1700 Fribourg (Switzerland), Fax: +41-26-300-9733, e-mail: Beat.Schwaller@unifr.ch

Received 10 September 2008; received after revision 15 October 2008; accepted 4 November 2008
Online First 16 December 2008

Abstract. Advances in the understanding of a class of Ca^{2+}-binding proteins usually referred to as "Ca^{2+} buffers" are reported. Proteins historically embraced within this group include parvalbumins (α and β), calbindin-D9k, calbindin-D28k and calretinin. Within the last few years a wealth of data has accumulated that allow a better understanding of the functions of particular family members of the >240 identified EF-hand Ca^{2+}-binding proteins encoded by the human genome. Studies often involving transgenic animal models have revealed that they exert their specific functions within an intricate network consisting of many proteins and cellular mechanisms involved in Ca^{2+} signaling and Ca^{2+} homeostasis, and are thus an essential part of the Ca^{2+} homeostasome. Recent results indicate that calbindin-D28k, possibly also calretinin and oncomodulin, the mammalian β parvalbumin, might have additional Ca^{2+} sensor functions, leaving parvalbumin and calbindin-D9k as the only "pure" Ca^{2+} buffers.

Keywords. Calbindin, calretinin, parvalbumin, oncomodulin, EF-hand, calcium-binding protein.

Introduction and "family relations": Ca^{2+}-binding proteins, EF hands, parvalbumin, calbindin-D9k, calbindin-D28k and calretinin

More than 50 years ago the first Ca^{2+}-binding protein (CaBP) of the EF-hand family was named parvalbumin (PV), based on its small size (parvus = small) and its albumin-like solubility [1]. The protein was isolated from carp muscle, where it is expressed at millimolar levels, and this preparation was used to obtain protein crystals that allowed the X-ray structure of the EF-hand domain to be deduced [2]. In general, an EF-hand domain consists of 29–30 amino acids: an α-helix, followed by a highly conserved stretch of 12 amino acids involved in chelating the Ca^{2+} ion and, finally, a second α-helix oriented approximately perpendicular to the first one. In the structure of PV, three such motifs, comprising six helical structures named A–F are present, and the X-ray structure of the most C-terminal motif, E-helix–Ca^{2+}-binding loop–F-helix, led to the name EF domain. Based on the fact that this structural motif can be represented by the index finger and the thumb of the right hand, while the bent middle finger represents the Ca^{2+}-binding loop, this structure is commonly referred to as an EF-hand domain (Fig. 1). Around the same time, two other family members were discovered by their ability to bind Ca^{2+} ions and by their expression being regulated by vitamin D: calbindin-D28k (CB-D28k) was first observed in the chicken duodenal mucosa [3], and supplying vitamin D to vitamin D-deficient rats induced a protein in the intestinal mucosa [4], later identified as calbindin-D9k (CB-D9k). Their names thus reflect the fact that they are proteins capable of binding Ca^{2+}, are induced by vitamin D and have apparent molecular masses of 28 and 9 kDa, respectively, as determined by denaturing SDS-polyacrylamide gel electrophoresis. Despite their similar names, they belong to entirely different subfamilies of EF-hand proteins and thus share little sequence homol-

ogy. CB-D28k (human gene symbol: *CALB1*) belongs together with calretinin (CR; *CALB2*) and secretagogin (*SCGN*) to the CALB family of proteins with six EF-hand domains, whereas CB-D9k is a member of the large S100 family (human gene symbol: *S100G*; for the classification, see [5] and for a recent review on the S100 family, see [6]). CR was initially identified as a protein band of 29 kDa present on Western blots using rat brain extracts that cross-reacted with an anti-CB-D28k antibody [7]. Based on the high homology with CB-D28k, also at the mRNA level, probing of a chick retina cDNA library under low-stringency hybridization conditions yielded clones containing the partial sequence of another protein that was named calretinin based on its origin (retina) of first detection and the close resemblance to CB-D28k [8]. The prototypical Ca^{2+} sensor calmodulin (CaM) was initially identified in 1970 as a protein, which activates cyclic nucleotide phosphodiesterase (for a review on early studies on CaM, see [9]). As more and more sequences from EF-hand proteins emerged, it was mainly Kretsinger and co-workers that specialized in categorizing family members according to sequence features. Their findings have been published since 1980 [10] and the latest classification dates from 1998 [5]. Analysis of the entire human genome has revealed 242 proteins containing EF-hand domains [11] and more than 600 have been identified altogether, from many different species [12]. Thus, the family may be considered as consisting of a finite known number of proteins, at least in humans and when applying the well-accepted search criteria of the conserved residues X, Y, Z, -Y, -X, -Z (for details, see Fig. 1). Besides the immunoglobulin superfamily, the EF-hand family of CaBPs is among the largest family containing a single motif. In general, EF-hand proteins have an even number of domains (2, 4, 6, 8) organized in pairs, but in mammals no EF-hand proteins with more than six domains have yet been detected. Few exceptions exist with proteins having an odd number of EF-hand domains, most notably PVs (α and β lineage, see below) and the family of penta-EF-hand proteins [13]. Knockout (KO) mice have been generated for the four proteins PV, CB-D9k, CB-D28k and CR that are the main focus of this review (Table 1) and this has helped in elucidating the function(s). Results obtained with these animals are described in the following sections.

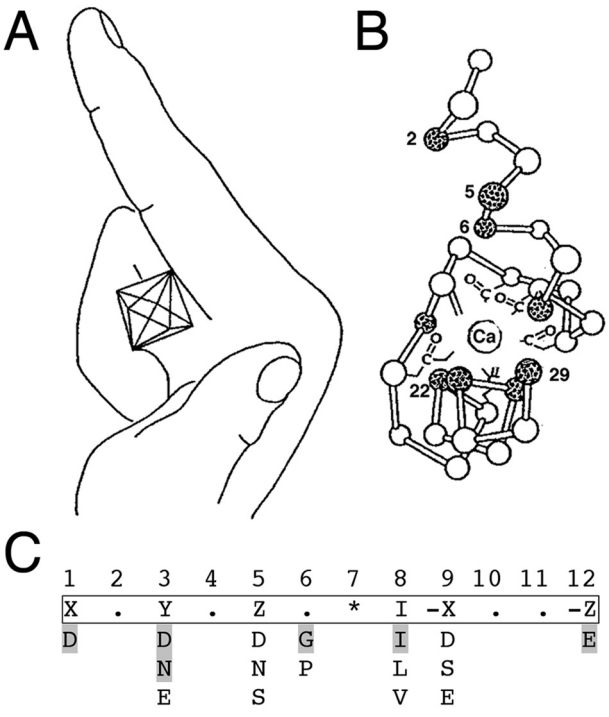

Figure 1. EF-hand domain motif. (*A*) The three-dimensional structure of the EF-hand motif can be visualized by the right hand: the index finger represents the E-helix (residues 1–10), the bent middle finger stands for the 12 amino acids of the canonical Ca^{2+}-binding loop (10–21), and the thumb signifies the F-helix (19–29). The seven oxygen ligands coordinating the Ca^{2+} ion are located at the seven corners of a pentagonal bipyramid (modified from [25]). (*B*) X-ray structure from the EF-domain of carp parvalbumin (modified from [2]). (*C*) The consensus sequence of the EF-hand Ca^{2+} -binding loop of 12 amino acids (boxed). X, Y, Z, and -Z are side-chain oxygen ligands, * (also termed -Y) indicates the backbone carbonyl ligand, and -X is a water ligand that is hydrogen-bonded to a loop residue. In position 8 (I) Ile, Val and Leu are the most common residues. At positions X and -Z, Asp and Glu are generally present, respectively; "." denotes any amino acid. Amino acids at positions 1, 3, 5, 6, 8 and 12 are the most highly conserved residues, in particular the ones shaded in gray. A comprehensive review on the structures and metal-binding properties of EF-hand domains has been published recently [240]. Data taken from [227] and PROSITE (http://www.expasy.ch/cgi-bin/nicedoc.pl?PDOC00018).

Ca^{2+} sensors vs Ca^{2+} buffers

Based on several characteristic features, EF-hand proteins are typically either classified as Ca^{2+} sensors or Ca^{2+} buffers [14, 15], but based on most recent results, the distinction between the two groups is starting to blur. A typical hallmark for sensors is their relatively large Ca^{2+}-dependent conformational changes often accompanied by exposure of hydrophobic surfaces allowing the interaction with specific ligands and subsequent regulation of downstream effectors (for a review, see [14]). The best-studied example of a Ca^{2+} sensor is the ubiquitously expressed CaM and still today, more CaM-dependent functions as well as CaM-modulated targets are being discovered (for recent reviews on CaM function, see [16, 17]). On the other hand, the ^{15}NMR relaxation studies on the typical buffer PV revealed the solution structure to be relatively rigid [18], and both Ca^{2+}-

Table 1. Transgenic mouse strains with altered Ca^{2+} buffer expression.

Protein (mouse gene name) [references]	Comments/ initial reported phenotype
Parvalbumin α (Pvalb) [61, 65, 68]	Constitutive KO. The muscle phenotype was first reported: changes in the dynamics of Ca^{2+} transients, *i.e.*, a slower initial decay in Ca^{2+} leads to a prolongation of the time required to attain peak twitch tension and to an extension of the half-relaxation time. In the brain, by delaying the buildup of residual Ca^{2+} in presynaptic terminals, PV modulates short-term synaptic plasticity, *i.e.*, it attenuates facilitation between stellate/basket cells and Purkinje cells as well as between PV-ir interneurons and hippocampal pyramidal cells.
Parvalbumin β (Ocm)	Not available at the time.
Calbindin-D28k (Calb1) [127]	Constitutive KO. Initial reported phenotype includes impaired motor coordination and changes in the Ca^{2+} signaling in Purkinje cell dendrites.
Calbindin-D28k (Calb1) [147, 148, 186]	Purkinje cell-specific KO. A similar impairment in motor coordination is observed as in the constitutive KOs indicating that cerebellar CB-D28k expression is responsible for the observed phenotype. Albeit changes in the time course and amplitude of fast Ca^{2+} transients after parallel or climbing fiber stimulation, no alterations in delayed metabotropic glutamate receptor-mediated Ca^{2+} transients and in LTD are observed.
Calretinin (Calb2) [74, 183, 184]	Constitutive KO. Basal synaptic transmission between the perforant pathway and dentate gyrus granule cells as well as at the Schaffer commissural input to CA1 pyramidal neurons is normal, yet LTP is impaired in the dentate gyrus and CR-/- mice show a mild impairment in motor coordination. In the cerebellum, excitability of granule cells is increased leading to an increase in Purkinje cell firing and synchrony and the occurrence of fast 160-Hz oscillation. CR-/- mice show a mild impairment in motor coordination.
Calretinin (Calb2) [188]	Selective expression of CR only in cerebellar granule cells, no CR expression in all other neurons. In alert mice, granule cell excitability and Purkinje cell firing behavior is normal, and the 160-Hz oscillations observed in constitutive CR-/- mice do not occur. With that, the motor phenotype is rescued and these mice show normal motor coordination.
Calbindin-D9k (S100 g) [166]	Constitutive KO. No overt phenotype with respect to Ca^{2+} homeostasis is observed likely due to compensatory molecular regulation mechanisms. An up-regulation of intestinal TRPV6 and PMCA1b during preweaning and renal Ca^{2+} transporters in adults may be responsible for essentially normal Ca^{2+} homeostasis.
Calbindin-D9k (S100 g) [164, 165]	A frame shift deletion in the S100G gene in the ES cell line E14.1 leads to a constitutional knockout. No evident phenotype with respect to viability, reproduction and serum Ca^{2+} levels is seen and also Ca^{2+} absorption from the intestine in response to D3 is normal.
TRPV6 (Trpv6) × **Calbindin-D9k** (S100 g) [167]	Constitutive KO by breeding of the two single KO strains. As in single KO mice TRPV6-/- and CB-D9k-/-, serum Ca^{2+} levels are normal, but in the absence of functional TRPV6, PTH levels are increased. Under low dietary calcium conditions, Ca^{2+} transport in the duodenum is less increased than in WT mice, but D3 administration to vitamin D-deficient KO (TRPV6, CB-D9k) and WT significantly increases duodenal Ca^{2+} transport, implying that active intestinal Ca^{2+} transport can occur in the absence of TRPV6, CB-D9k or both.
TRPV5 (Trpv5) × **Calbindin-D28k** (Calb1) [162]	Constitutive KO by breeding of the two single KO strains. TRPV5-/- CB-D28K-/- mice show hypercalciuria, both under high or low calcium diets, as also seen in TRPV5-/-, but not CB-D28k-/- mice. In the absence of TRPV5, CB-D9k is up-regulated in the kidney and results in intestinal Ca^{2+} hyperabsorption due to elevated CB-D9k and TRPV6 expression levels. These effects are not present in single KO CB-D28k-/- mice.
Parvalbumin (Pvalb) × **Calbindin-D28k** (Calb1) [76, 213]	Constitutive KO by breeding of the two single KO strains. Purkinje cell dendritic spines of double KO mice are longer and both spine surface and volume are larger. An attenuated effect is also seen in CB-D28k-/-, but not in PV-/- mice. Alert mice show 160-Hz oscillations in the absence of one or the other protein and alterations in Purkinje cell firing properties, the biggest differences compared to WT mice are seen when both proteins are absent.
Parvalbumin (Pvalb) × **Calretinin** (Calb2) [230]	Constitutive KO by breeding of the two single KO strains. Epileptogenesis using a kainate model of mesial temporal lobe epilepsy and also long-term seizure-related alterations of the cytoarchitecture of the hippocampal formation are not different compared to WT mice.
Calbindin-D28k (Calb1) × **Calretinin** (Calb2) [73]	Constitutive KO by breeding of the two single KO strains. Alterations in Purkinje cell firing properties, but not their intrinsic somatic excitability; cerebellar oscillations are observed that are slightly different than the ones seen in single KO mice.
Calbindin-D28k (Calb1) × **Calretinin** (Calb2) x **Parvalbumin** (Pvalb)	Constitutive KO by breeding of the three single KO strains. The hearing phenotype is currently being investigated, since all three proteins are expressed in inner hair cells.
Thy-PV [218]	Ectopic expression of PV under the control of the Thy-1 promoter. Ca^{2+} transients elicited by activation of Ca^{2+}-permeable AMPA receptors with kainic acid in cultured motor neurons are attenuated in Thy-PV mice and partially protect these neurons from cell death.

Table 1 *(Continued)*

Protein (mouse gene name) [references]	Comments/ initial reported phenotype
CaMKII-PV [231]	Ectopic expression of PV under the control of the CaM-dependent kinase II promoter. The increase in $[Ca^{2+}]_i$ in CaMKII-PV motor neurons mediated by immunoglobulins from ALS patients is decreased. Mutant SOD1 (mSOD1) transgenic mice, an animal model of familial ALS, bred with CaMKII-PV mice show reduced motor neuron loss and have a delayed onset of the disease.
PV-EGFP [232]	In this transgenic reporter strain, the enhanced green fluorescent protein (EGFP) is expressed under the control of the Pvalb promoter and EGFP expression is observed in cells normally expressing PV ("PV-ir" neurons, fast-twitch muscles, renal epithelial cells in DCT1)

binding and Ca^{2+}-release only induce relatively small conformational changes most often confined to the Ca^{2+}-binding loop itself or to the close vicinity of the EF-hand domain. Thus, the predominant function of PV is assumed to lie in the control and/or modulation of the spatio-temporal aspects of intracellular Ca^{2+} ($[Ca^{2+}]_i$) signals (reviewed in [19–21]). These signals are very short-lived, especially in excitable cells such as neurons or muscle cells, in the range of few to hundreds of milliseconds, and are termed Ca^{2+} transients. Depending on the cell type and the spatio-temporal aspects, various names are given to these Ca^{2+} transients; waves, spikes, sparks, puffs, quarks, just to name a few; for details on the "taxonomy of elementary cellular Ca^{2+} signaling events", see [22]. In the following chapters, I discuss how different Ca^{2+} buffers modulate such Ca^{2+} transients and their effects on cell physiology. Evidently even Ca^{2+} sensors are able to modulate Ca^{2+} transients, when present at high enough concentrations. I focus mainly on recent findings on the Ca^{2+} buffers PV (α and β lineage, the latter also called oncomodulin, OM), CB-D9k, CB-D28k and CR. Several extensive reviews on the classical Ca^{2+} sensors including CaM [16, 17], the S100 family [6] and the neuronal calcium sensor (NCS) family [23, 24] have been published recently. I also discuss the possible dual roles of CB-D28k and CR, as buffers as well as sensors.

Relevant parameters to describe the properties of Ca^{2+} buffers/sensors

In many initial studies, Ca^{2+} affinities, often represented by the dissociation constant $K_{D,Ca}$, were a major focus of research on CaBPs as well as how changes in the essential amino acids of the Ca^{2+}-binding loop affect the binding properties (for review, see [25, 26]). Also, with the help of intracellular fluorescent Ca^{2+} indicators, it became clear that, under resting conditions, $[Ca^{2+}]_i$ is in the order of 50–100 nM in almost all cells, including neurons and muscle cells. Based on the reported CaBP dissociation constants ($K_{D,Ca}$) that are mostly in the low micromolar range, most of the Ca^{2+}-buffering protein molecules are evidently in the Ca^{2+}-free form under conditions of a resting (non-activated) cell. Yet following a rise in $[Ca^{2+}]_i$ due to Ca^{2+} influx or Ca^{2+} release from internal stores, CaBPs will modulate the spatio-temporal aspects of Ca^{2+} signals. These Ca^{2+} transients in excitable cells are often of short duration (in the range of 10 to several 100 ms) and highly localized, e.g., within the presynaptic terminal of axons or in sites flanking the Z-lines and colocalized with T-tubules in muscle fibers [27]. The most important parameters relating to this modulating function include: (a) the cytosolic concentration of the buffer molecules, (b) their affinity for Ca^{2+} and possibly other metal ions (*e.g.*, Mg^{2+}), (c) the kinetics of Ca^{2+} binding and release, and (d) their mobility inside cells (for details, see [20]). For practical reasons, the Ca^{2+}-binding ratio of endogenous buffers, *i.e.*, the ratio of buffer-bound Ca^{2+} changes over free Ca^{2+} changes ($\kappa_S \sim [Ca^{2+}\ \text{buffer}] / K_{D,Ca}$), according to the single compartment and linear approximation model [28, 29], is often used as a measure to express the buffering capacity of various cell types. In particular, if the identity and property of the various CaBPs within a cell type are not known precisely. Motor neurons are characterized by very low buffering ($\kappa_S < 50$ [30]), "typical" neurons have values in the order of 60–200 [31], and Purkinje cells expressing high levels of CB-D28k and PV are characterized by very high κ_S values in the order of 900–2000 [32].
For none of the proteins discussed in this review have all four parameters mentioned above been determined with precision *in vivo*. In the following chapters, I summarize the current knowledge about specific Ca^{2+} buffers with respect to the above-explained parameters and how this affects cell physiology as well as pathologies where these proteins might be implicated. New findings with respect to protein structure, Ca^{2+}-binding properties, localization, putative function and briefly, the involvement in pathologies are discussed.

Parvalbumins (α and β lineage)

Structural aspects

Although the X-ray structure of PV was already published in 1973 [2], not all secrets have been revealed. PV (mol. mass ~12 kDa) is a remarkable exception in the family of EF-hand proteins in several ways. It is one of the few proteins with three EF-hand domains, albeit only two functional ones with respect to metal binding. The most N-terminal AB site is unable to bind Ca^{2+} ions due to strong deviations from the consensus Ca^{2+}-binding loop sequence, but nonetheless the AB domain is necessary for the stability of PV [33]. Furthermore, the CD and EF domains also have peculiar properties, such that they bind Ca^{2+} with high affinity and Mg^{2+} with a moderate affinity in a competitive manner (dissociation constants: $K_{D,Ca} \leq [Ca^{2+}]_i$, *i.e.*, ~5–100 nM and $K_{D,Mg} < [Mg^{2+}]_i$, *i.e.*, ~5–500 μM), and are thus termed Ca^{2+}/Mg^{2+} mixed sites (for details, see [25]). Thus, in the cytoplasm of a "resting" cell (*e.g.*, fast-twitch muscle fibers, neurons) with reported intracellular Mg^{2+} concentrations of 0.5–1 mM [34, 35], the mixed Ca^{2+}/Mg^{2+} sites of PV are occupied largely by Mg^{2+} (80–90 %), which needs to dissociate before Ca^{2+} binding can occur. Due to this mechanism, *i.e.*, the rate of Ca^{2+} binding being determined by the rather slow Mg^{2+} off-rate, PV is considered to be a "slow" buffer and the kinetics of Ca^{2+} binding can be closely mimicked by the slow synthetic buffer EGTA. As in most proteins with an even number of EF-hand domains, the two connected domains CD and EF in PV also form a pair consisting of two helix-loop-helix regions linked by a short stretch of five to ten amino acid residues. In both sites the Ca^{2+} ion is coordinated by seven ligands, best described as a pentagonal bipyramid with the Ca^{2+} ion sitting in the center and the ligands at the corners of this structure (Fig. 1) [36]. While the crystal structure of PV was known early on [2], in the last few years, more structures of PV in solution from different species or β PV structures have been published [37]. They include NMR studies on C and N relaxation of the Ca^{2+}-loaded pike and rat PV [18], the apo (metal-free form) of rat α PV [38] and β PV [39]. The results from these studies can be briefly summarized as: (i) the Ca^{2+}-loaded EF-hand domains of rat α PV as well as the linker region connecting the CD and EF domain are extremely rigid structures in comparison to those in CaM or CB-D28k and also the N and C termini of PV have a low intrinsic mobility [18]. (ii) The solution structures of rat α PV in the apo- and Ca^{2+}-loaded forms are quite similar, structural differences are mainly observed in the loop region, and thus Ca^{2+}-binding does not require major structural rearrangements [38]. (iii) The same holds also true for the Ca^{2+}/Mg^{2+} mixed site (EF) in rat β PV (dissociation constants: $K_{D,Ca}$ ~45 nM and $K_{D,Mg}$ ~250 μM), while the CD site, which is a Ca^{2+}-specific site ($K_{D,Ca}$ ~0.6 μM, for details, see [40] and below), undergoes significant structural alterations when Ca^{2+} is removed from β PV. This includes a rearrangement of the two helices in the CD site as well as a reorganization of the hydrophobic core and remodeling of the interface between the non-functional AB and the CD-EF domains [39]. Thus, α– and β PV not only differ in the Ca^{2+} binding affinity of their CD site, the global rigidity of α PV makes this molecule a prime candidate as a Ca^{2+} buffer, while the Ca^{2+}-induced conformational changes in β PV may hint towards additional functions, possibly also as a Ca^{2+} sensor (see below).

Another essential parameter for Ca^{2+} buffers is their intracellular mobility. The diffusion coefficient (D) of PV in aqueous solution (~140 $\mu m^2/s$ [41, 42]) is clearly larger than in the myoplasm of skinned frog muscle fibers (~40 $\mu m^2/s$ [43]) and in dendrites of cerebellar Purkinje neurons, the latter determined by two-photon fluorescence recovery after photobleaching (FRAP; 43 $\mu m^2/s$ [44]). In other cellular compartments of the same Purkinje neurons (soma, nucleus, axon), the diffusional mobility is further decreased to approximately 11 $\mu m^2/s$ [45]. Yet in all preparations, when the mobility of PV is compared to the mobility of a dextran molecule of a similar size (approx. 10 kDa) that is expected not to specifically interact with intracellular constituents, the mobility of the two molecules decrease in a similar way. Thus, differences in PV mobility in various cell compartments can be principally attributed to differences in cytoplasmic viscosity or tortuosity; results from all experiments on the mobility of PV are consistent with the model of PV being a mobile molecule freely diffusing in the various cellular compartments of PV-expressing cells.

Nomenclature of genes and proteins of the PV family

Certain confusion in the literature has arisen from the fact that in different species, other genes with close homology to α PV (human gene name *PVALB*) exist. The encoded proteins consist of 107–113 amino acids and have apparent molecular masses of 12 000–14 000. According to the amino acid sequence, isoelectric point and also Ca^{2+}-binding characteristics, PVs from different species have been classified into α and β lineages (for details see [25]), and in different species completely different names were given to β PVs. In mammals β PV is known under the name oncomodulin (human gene symbol *OCM*). The proteins encoded by the two β PV forms in birds are either called avian thymic hormone (ATH), thymus-specific PV or thymus-specific antigen T1 (gene name:

PVALB), while the other form is named oncomodulin or PV 3 (CPV3; gene name: OCM). Unfortunately, the chicken α PV has also PVALB as a gene symbol. The rat β PV (oncomodulin; OM) was first detected in hepatic solid tumors [46]. Based on the strong sequence homology to CaM and its apparent selective expression in tumor tissue, the protein was named OM. OM expression was later observed in the cytoplasm of cytotrophoblasts of the placenta and in early embryos of rodents and other mammals [47]. The other β PV form in chicken was first detected as a thymus-specific antigen T_1 in the chicken [48] and was later named avian thymic hormone (ATH) based on its ability to stimulate differentiation of T cell precursors and to enhance the proliferative activity of certain mitogens [49, 50]. However, the most prominent expression of β PV (OM), initially called CBP-15 in the guinea pig, is in the inner ear, specifically restricted to outer hair cells (OHC; [51]). Interestingly, α PV is expressed in both inner hair cells (IHC) and OHC in the organ of Corti [52]. Also the expression of α and β PV is regulated differently; β PV expression only occurs after efferent innervation starting from postnatal day 2 (P2) to P4 and in organ cultures isolated before efferent innervation of OHC, β PV expression fails to develop. In contrast, α PV expression in IHC and OHC appears to be independent of efferent innervation. A detailed study by Hackney and co-workers [53] determined the concentrations of all known Ca^{2+}-buffering proteins (α PV, β PV, CB-D28k, CR) in IHC and OHC also during development. The α PV concentration in IHC and OHC from rat and mouse is around 100–300 μM and tenfold higher concentrations of β PV (2–3 mM) are found in OHC. A comprehensive review on Ca^{2+} signaling mechanisms in hair cells, in particular the ribbon synapse has been published recently [54].

Ca^{2+}/Mg^{2+} mixed sites vs Ca^{2+}-specific sites

Many studies have attempted to elucidate the mechanism by which a Ca^{2+}/Mg^{2+} mixed site (*e.g.*, the CD site in α PV) can be converted into a Ca^{2+}-specific site (*e.g.*, the CD site in β PV). This involved the swapping of the entire CD domain from one protein to the other [55] or site-specific changes of amino acid residues in the CD loop of rat PV with the ones present in rat OM [56]. The results from these studies indicate that the specificity (Ca^{2+}/Mg^{2+} mixed vs Ca^{2+} specific) resides within the whole CD domain, not only in the Ca^{2+}-binding loop. Finally, it was attempted to convert the non-functional AB domain Ca^{2+}-binding loop of PV and OM into a functional one by replacing the 10-residue-long nonfunctional loop in the AB by a canonical 12-amino acid loop [33]. Yet, the introduced mutations did not "reactivate" the AB domain, but instead increased the cooperativity between the two functional CD and EF domains ($n_H = 2$). Thus, the main function of the AB domain is likely to provide conformational stability of metal-free PV.

Functional aspects of PV and OM

The delayed Ca^{2+}-binding properties of PV together with its large concentration (up to 3 mM) in fish muscle led to the early hypothesis that PV might act as a relaxation factor by facilitating Ca^{2+} transport from the myofibrils to the sarcoplasmic reticulum [57, 58] (for a review on the role of PV in muscle, see [59]). A direct role for PV in muscle relaxation was shown by injecting PV cDNA into the slow-twitch muscle *soleus* (SOL) of a rat, where the speed of relaxation is significantly increased, while contraction times are not affected [60]. The opposite is seen in PV KO mice (PV-/-, systematic name $Pvalb^{tm1Swal}$; Table 1): half-relaxation rates of an electrically induced single twitch in fast-twitch muscles, *tibialis anterior* (TA) are slower in the absence of PV [61]. That is, PV is too slow to affect the rapid rise in $[Ca^{2+}]_i$ occurring during the contraction phase, but increases the initial rate of $[Ca^{2+}]_i$ decay. Yet, under prolonged tetanic contraction, PV saturates with Ca^{2+} and acts as a transient Ca^{2+} source, prolonging the $[Ca^{2+}]_i$ decay and also the relaxation phase [62]. The effects of PV on $[Ca^{2+}]_i$ decay performed in PV-injected chromaffin were used to determine both the K_D and the kinetic parameters of Ca^{2+}- and Mg^{2+}-binding with high accuracy [63] (Table 2). PV considerably increases the initial rate of $[Ca^{2+}]_i$ decay (Ca^{2+}-binding phase), followed by a prolongation of the transient at later times (Ca^{2+}-releasing phase) yielding a bi-exponential $[Ca^{2+}]_i$ decay. Such a bi-exponential decay is seen in cultured PV-containing hippocampal interneurons *in vitro*, but not in excitatory neurons devoid of PV expression [31]. This "signature" of PV is also seen in PV-expressing neurons in slice cultures, both pre- and post-synaptically. The results obtained from PV-/- as well as other CaBP-deficient mice have been reviewed previously [21, 64] and are briefly summarized here. At the synapses between stellate/basket cells and Purkinje cells paired-pulse depression (PPR ~0.85) in wild-type (WT) mice changes to facilitation (PPR ~1.17) at 30 ms interspike interval (ISI) in PV-/- mice [65], due to the higher residual $[Ca^{2+}]_i$ in the presynaptic terminals, *i.e.*, interneuron varicosities [66]. The effect of PV is most pronounced after short ISI (30 ms) when $[Ca^{2+}]_i$ decay curves in the presence or absence of PV show the largest differences. Not only the increase in initial $[Ca^{2+}]_i$ decay is of importance, but also the slow decay component, *i.e.*, PV, acting as a Ca^{2+} source, leads to a robust PV-dependent, delayed transmitter release at interneuron-interneuron synap-

ses subsequent to presynaptic bursts of action potentials [66]. Despite the fact that hippocampal PV-expressing interneurons, axo-axonic and basket cells [67] are likely involved in similar mechanisms as cerebellar interneurons, no differences in paired-pulse modulation between control and PV-/- mice are apparent; the expected "PV effect" is only seen when pulse trains at 33, 50 and 100 Hz are delivered indicative of more efficient presynaptic Ca^{2+} extrusion mechanisms in hippocampal PV interneurons [68]. Evidently, the "steady-state" $[Ca^{2+}]_i$ level during a series of burst-like action potentials (AP) depends upon $\Delta t/\tau$; Δt being the time interval between APs and τ the Ca^{2+} relaxation time constant of individual Ca^{2+} transients. At stimulation frequencies of 20 Hz or less (ISI >50 ms), both in the presence and absence of PV, the decay in $[Ca^{2+}]_i$ is fast enough to prevent buildup of residual Ca^{2+} and becomes manifest only at higher frequencies (>30 Hz). Interestingly, the relative effect of PV in preventing facilitation is strongest at ~33 Hz, within the range of gamma frequency (30–80 Hz) oscillations. The maximum power of gamma oscillations *in vitro* recorded with dual field potential recordings in area CA3 from PV-/- mice is higher than in control mice and can be explained by an increased facilitation of GABA release at sustained high frequencies. The physiological consequences of this effect at the network level are discussed below. Although principally expressed in GABAergic interneurons, PV is also present at a large excitatory nerve terminal in the auditory brainstem, the calyx of Held, where presynaptic Ca^{2+} plays a crucial role in short-term plasticity. This synapse is characterized by a very fast Ca^{2+} decay (τ_{fast} ~30 ms) that slows down during presynaptic whole-cell recordings as the result of washing out of (an) endogenous mobile Ca^{2+} buffer(s) (*e.g.*, PV). The loss of these buffers only marginally increases the amplitude of the $[Ca^{2+}]_i$ transient, indicative of a "slow" buffer being responsible for the effect. Addition of PV in the recording pipette restores both the fast decay kinetics of $[Ca^{2+}]_i$ and paired-pulse facilitation [69]. Results from the "run-down" whole-cell recordings in rat neurons are very similar to recordings made in PV-/- neurons after brief preloading with the Ca^{2+} indicator fura-6F, further supporting the role of PV in accelerating the decay of spatially averaged $[Ca^{2+}]_i$ and paired-pulse facilitation. The role of postsynaptic PV was addressed in PV-/- Purkinje cells by analysis of the climbing fiber-mediated Ca^{2+} transients in spiny dendrites [70]. As in other neurons, the Ca^{2+} peak amplitude is not significantly altered, while the biphasic nature of the $[Ca^{2+}]_i$ decay – the typical signature of the slow binding kinetics of PV – is greatly reduced in the absence of PV. What are the global consequences of eliminating PV from this network of inhibitory neurons often critically involved in strong perisomatic inhibition? Previously, it was hypothesized that a change in the inhibitory activity of PV neurons in the neocortex may be a major mechanism underlying epileptic seizures [71]. Although PV-/- mice show no signs of spontaneous epileptic activity, pentylenetetrazole (PTZ)-induced seizures, albeit delayed, are more severe in PV-/- than in WT mice [72]. This indicates that the inhibitory effect exerted by the subpopulation of "PV interneurons" of the cerebellum and hippocampus is enhanced in the brain of PV-/- mice. In the hippocampus, the absence of PV facilitates the $GABA_A$ergic current reversal induced by high-frequency stimulation and thereby the proconvulsive GABA-mediated depolarizing postsynaptic potential. In summary, PV plays a major role in regulating the local inhibitory effects exerted by GABAergic interneurons on principal neurons.

PV deficiency also affects cerebellar function(s), likely involving the entire circuit. As in CR-/- and CB-D28k-/- mice [73], the absence of PV induces 160-Hz oscillations sustained by synchronous, rhythmic-firing Purkinje cells aligned along the parallel fiber axis. Cell firing alterations include a decrease in complex spike duration and spike pause, and an increase in simple spike firing rate (for details, see [74]). At the behavioral level, these changes are likely responsible for the very mild locomotor phenotype, *i.e.*, an impairment of motor coordination/motor learning [75]. Note that all the reported changes are also seen in CB-D28k-/- mice and the highest magnitude of most changes observed at the cellular level are also manifested as a greater impairment in motor coordination/learning in CB-D28k-/- mice [75, 76].

PV and neurological diseases?

Many studies have reported alterations in the expression of CaBPs including PV in various brain regions of postmortem patients with specific pathologies including Alzheimer's, Huntington's and Parkinson's disease, various types of ataxia, and disorders such as epilepsy, schizophrenia, bipolar disorder and depression (for a review, see [64, 77, 78]). Also changes in PV expression have been reported in animal models of these diseases. Yet in many cases, authors report correlations such as "down-regulation of PV in the area XY of Z patients", but most often it is not investigated whether (a) PV expression is reduced in this neuron subpopulation, (b) this subpopulation of neurons have degenerated, or, moreover, (c) whether PV is involved in the observed changes. Within the last few years many reports of this type have appeared, but unfortunately little knowledge on the function of CaBPs can be gleaned from these studies.

Table 2. Properties of selected Ca^{2+}-binding proteins in comparison to the synthetic buffers EGTA and BAPTA (adapted from [64]).

	EGTA	BAPTA	α PV	β PV (OM)	CB-D9k	CB-D28k	CR
Ca^{2+} binding sites (functional)	1 (1)	1 (1)	3 (2)	3 (2)	2 (2)	6 (4)	6 (5)
Ca^{2+}-specific /mixed Ca^{2+}/Mg^{2+} sites	1/0	1/0	0/2	1/1	2/0	4/0[a]	5/0
$K_{D,Ca}$ (nM)	70–150	160	4–9[b]	Mixed: 42–45[d] Ca^{2+}-specific: 590–780[d]	K_{D1} ~200–500[e] K_{D2} ~60–300	High aff. (h)[f] K_{D1} ~180–240 medium aff. (m) K_{D2} ~410–510	$K_{D(T)}$ 28 μM[g] $K_{D(R)}$ 68 $K_{D(app)}$ 1.4 μM EF5: 36 μM
$K_{D,Mg}$			~30 μM[b]	160–250 μM[d]		714 μM[a]	4.5 mM[h]
$K_{D,Ca(app)}$ (nM) at $[Mg^{2+}]$ of 0.5–1 mM			150–250[c]	230–310 nM[c]			
$k_{on,Ca}$ ($\mu M^{-1} s^{-1}$)	3–10[f,i]	100–1000[f,i]	6[b]		up to 1000[e]	h sites ~12[f] m sites ~82	2 T sites: 1.8 [g] 2 R sites: 310 site EF5: 7.3
$k_{on,Mg}$ ($\mu M^{-1} s^{-1}$)			0.1–1[c]				
$k_{off,Ca}$ (s^{-1}) = $K_{D,Ca}$ * k_{on}	0.5–1.5	16–160	0.9–1.03[j]			h sites: 2–3[f] m sites: 34–42	T sites ~50 [g] R sites ~20 site EF5 ~260
$k_{off,Mg}$ (s^{-1})			3.42[j] 11–25[j]				
Cooperativity			no[k]	? yes[l]	yes[m]	yes n_H ~1.1–1.2[a]	yes n_H ~1.3–1.9[g]
$D_{Cabuffer}$ ($\mu m^2 s^{-1}$)	200 [n]	200 [n]	37–43[o] ~11			>100[p] ~25	~25[p]

a Based on the affinity for Mg2+ [126], the sites may also be considered as mixed sites, but the Ca2+/Mg2+ antagonism is much less pronounced than in the two and one mixed sites of α and β PV, respectively. b [233]. c KD and kon for PV are highly dependent on [Mg2+] – the values stated are estimates at physiological cytosolic [Mg2+] (0.6–0.9 mM). d [40]. e The reported value represents the diffusion limit, assuming a maximal Ca2+ diffusion rate of ~200 μm2 s–1 [104, 234]. f The four functional sites of CB can be classified as either medium-affinity (m) sites with fast binding kinetics or high-affinity (h) sites with slower binding kinetics [125]. The model gave equally good results with CB-D28k having two high and two medium sites or three high and one medium site. Cooperativity of Ca2+-binding sites was not included in the model to calculate the different parameters. g For details, see Fig. 3 and text [174]. h [171]. i [235]. j [57, 63, 236]. k PV has two essentially identical Ca2+-binding sites with nH close to 1. l [90]. m [237]. n Values for EGTA and BAPTA are based on the reported mobility (283 μm2 s–1) of IP3 [238]. o The diffusion coefficients DCabuffer for PV are very similar in muscle myoplasm (37 μm2 s–1) [43] and in dendrites of Purkinje cells (43 μm2 s–1) [44], but are smaller in the soma and axons (~12 μm2 s–1) [45]. p While the mobility is rather high in water [239], mobility of CB-D28k inside Purkinje cell dendrites is only 26 μm2 s–1 [128], clearly slower than PV. The mobility of CR is assumed to be similar as for CB-D28k based on the similar molecular mass of CB-D28k and CR.

Role of PV in kidney function

Besides muscle and brain, PV is also expressed in the kidney. In the rat, PV expression occurs in part of the distal convoluted tubule and proximal collecting duct [79]. More recent studies in the mouse revealed that PV is essentially localized to the early distal convoluted tubule (DCT1) that plays an essential role in NaCl reabsorption, where it colocalizes with the thiazide-sensitive Na^+/Cl^- cotransporter (NCC; for a general review on transcellular Ca^{2+} and Na^+ transport pathways in the murine distal nephron, see [80]). A significant overlap exists between PV expression and the Mg^{2+} channel involved in renal Mg^{2+} absorption, TRPM6 [81]. Increased diuresis and kaliuresis at baseline together with higher aldosterone levels and lower lithium clearance are seen in PV-/- mice [82]. Unexpectedly, acute furosemide administration does not increase calciuria; calciuria is increased only after NaCl supplementation, both at baseline and after furosemide treatment. In PV-/- kidney, expression of NCC is down-regulated. Overexpression of PV in mouse DCT cells *in vitro* induces endogenous NCC expression, suggesting that PV could act as a Ca^{2+}-dependent modulator of NCC expression levels. The finding that PV-/- mice have a positive Ca^{2+} balance and increased bone mineral density were interpreted to be related to NCC down-regulation, as a similar phenotype is seen in patients and mice having NCC deficiency, but could hint also that homeostatic mechanisms involving up-regulation of CB-D9k take place when PV is missing (for additional details, see also '*Transgenic mice used to study the "Ca^{2+} homeostasome" in renal and intestinal Ca^{2+} regulation*' below).

Regulation of PVs

Different factors regulate PV expression in both muscle and neurons. PV is regulated by estrogen *via* estrogen-receptor (ER) β. Expression of PV is increased in males and decreased in female ERβ-/-

muscles [83]. Interestingly, ERβ is strongly colocalized with PV-immunoreactive neurons in many brain regions (cortex, amygdala, basal forebrain and hippocampus) [84]. Two other factors implicated in the regulation of PV expression are electrical activity and light. Both chronic low-frequency stimulation of fast-twitch muscles [85] or denervation [86] lead to a significant decrease in PV expression, indicating that PV expression is under the control of fast-type motor neuron activity. Circadian variation of PV expression is observed in AII amacrine neurons of the rat retina [87] and also in the ciliated ependymal layer of the third ventricle at the level of the suprachiasmatic nuclei (SCN) [88]. Light exposure during late subjective night decreases PV staining in the cilia. Also in hair cells, expression of PV and OM is likely regulated during cochlear development and may be influenced by efferent innervation [52].

OM, initially detected in rat kidney tumors and derived cell lines, is present in the organ of Corti, the auditory receptor organ [51] and in gerbil, rat and mouse OM is exclusively expressed in cochlear OHCs [89]. A recent report showed that OM might act as a potent macrophage-derived growth factor for retinal ganglion cell (RGC) regeneration [90], indicating also a Ca^{2+} sensor role. OM binds to rat RGCs with high affinity in a cyclic AMP (cAMP)-dependent manner and stimulates more extensive axon outgrowth than other known trophic agents. An OM-dependent activation of cAMP phosphodiesterase (increased cAMP hydrolysis) has been reported [91]. Thus, it was suggested that OM is a new growth factor for neurons of the mature central and peripheral nervous systems. The latter finding was challenged recently, since (a) OM was reported to be not significantly expressed in primary macrophages, (b) intraocular OM levels did not increase after lens injury or zymosan treatment, and (c) strongly reducing macrophage invasion into the inner eye increased, not decreased axon regeneration into the optic nerve [92]. Thus, the role of OM as a putative neurotrophic factor is a novel exciting topic, but it is certainly too early to make any conclusive statements. An action as a hormone, *i.e.*, to promote immunological maturity in chicken bone marrow cells in culture, was also reported for the second β lineage type PV, called avian thymic hormone (ATH) [93]. ATH has also two Ca^{2+}/Mg^{2+} mixed sites similar to the "muscle and neuron"-type PV [94] and unlike OM that contains a Ca^{2+}-specific and a mixed Ca^{2+}/Mg^{2+} site. Since the ATH amino acid sequence is very similar to reptile (turtle, salamander and frog) β-type PVs, the authors proposed, "the evolutionary appearance of the warm-blooded reptiles was accompanied by recruitment of the β PV isozyme for promotion of lymphocyte maturation" [95]. The chick ortholog of OM, CPV3, is also expressed in thymus tissue. Further evidence that CPV3 is an OM isoform was provided by flow-dialysis measurements indicating that the Ca^{2+}-binding domains are not equivalent [96]. Both CPV3 and ATH are produced by epithelial cells in the thymic cortex of chickens. ATH circulates in the blood on a 5-day cycle and stimulates the development of cell-mediated immunity, further evidenced by an enhanced acute graft-*versus*-host reaction [97].

Calbindin-D9k

Structural and general aspects of CB-D9k

Since its discovery in 1967 [4], CB-D9k has served as a most useful model EF-hand protein. It is the smallest one with an EF-hand pair consisting of a "canonical" EF-hand domain with a Ca^{2+}-binding loop of 12 amino acids (EF2) and a non-canonical (also termed "pseudo EF-hand") Ca^{2+}-binding loop comprising 14 amino acids (EF1), typical for the S100 family proteins [6]. In contrast to the canonical loop, where Ca^{2+} binding occurs mainly *via* carboxyl side chain groups (Fig. 1), most of the ligands chelating the Ca^{2+} ion in the non-canonical loop of the S100 family proteins are backbone carbonyl groups [98]. Structural data obtained by X-ray, NMR [99, 100] and electrospray ionization mass spectrometry [101] methods together with the production of mutants with specific amino acid substitutions have revealed the most important structural features. The four α-helical regions are organized in two EF-hand domains joined by a linker region of ten amino acids and between the two Ca^{2+}-binding loops a short β-type interaction exists [102]. When artificially cleaving the protein into two halves, the Ca^{2+}-binding rates of the individual subdomains are several orders of magnitude lower than for the corresponding sites in the intact protein, indicating that EF-hands organized in tandem domains are the functionally relevant structures ([103], for a review, see [98]). The two EF-hand domains bind Ca^{2+} with similar affinities and positive cooperativity [104], also in the presence of physiological Mg^{2+} concentrations [105]. The overall Ca^{2+}-induced conformational change in CB-D9k is much less pronounced than in the typical sensor CaM, an argument in favor of CB-D9k mainly serving a role as a Ca^{2+} buffer compared to functioning as a Ca^{2+} sensor [106]. In rat kidney, CB-D9k is expressed in the loops of Henle and the distal convoluted tubule. In the collecting duct CB-D9k is restricted to the intercalated cells [107]. In the immunoreactive cells, labeling was found to be strongest along the basolateral membrane, but until now, no evidence for CB-D9k either interacting with membrane constituents or with

any other molecule has been presented. Thus, the "selective" staining of CB-D9k along the basolateral membrane might be an artifact for various reasons, *i.e.*, better fixation of the small CB-D9k molecule in the dense network of proteins on the inner surface of the basolateral membrane. Also binding of antibodies to their target CaBP is typically sensitive to the metal-binding status [108, 109] and may not be identical throughout the cell. Unlike for PV (for details see above), the mobility of CB-D9k in the various cells expressing this protein has not been reported so far, but based on the absence of identified binding partners and rather minor Ca^{2+}-dependent conformational changes, CB-D9k is assumed to be a freely mobile molecule, the mobility likely determined by the viscosity and/or tortuosity of the cytoplasmic compartment. An analysis of the mouse kidney revealed CB-D9k to be strongly expressed in distal convoluted tubules [110], more precisely in the late distal convoluted tubules and the connecting tubules (J. Loffing, personal communication) and thus highly colocalized in the same structures previously reported to express the epithelial Ca^{2+} channel TRPV5 (Fig. 3 in [80]). In the mouse intestine, strong expression of CB-D9k is restricted to the first 2 cm of the duodenum [111].

Functional aspects of CB-D9k

The regulation of CB-D9k expression by $1,25(OH)_2$ vitamin D3 (D3) led to the initial discovery of this protein in intestine [4], but other ways of regulation were identified in other tissues (for a comprehensive review on CB-D9k, see [112]). A functional estrogen-responsive-like element located at position +51 from the transcriptional initiation site in the rat gene sequence (S100G) is responsible for the estrogen-mediated expression of CB-D9k in the uterus [113]. A screen for estrogen-responsive genes in the rat pituitary cell line GH3 revealed the CB-D9k mRNA to be up-regulated almost 100-fold after 17-β-estradiol (E2) treatment [114]. Interestingly, the other strongly up-regulated mRNA was the one corresponding to the PV (PVALB) gene. Uterine CB-D9k mRNA levels are also increased in rats treated with xenobiotic agents acting as endocrine disruptors [115] *via* an ER-dependent pathway. Most recently, a non-classical pathway involving NF-κB was shown to contribute to elevated CB-D9k mRNA levels in GH3 cells [116] *via* an NF-κB-responsive element -848 to -834 from the transcriptional start site in the rat CB-D9k promoter. In mouse primary renal tubular cells, CB-D9k mRNA is also positively modulated by parathyroid hormone (PTH), acting synergistically with D3 [117]. Besides, endocrine regulation, intestinal CB-D9k is also regulated by Mg^{2+}; in rats fed a low Mg^{2+} diet, CB-D9k concentration increases, while at high Mg^{2+}, CB-D9k remains unchanged [118]. Renal CB-D28k levels are not affected by the low Mg^{2+} diet, but are lower in animals fed a high Mg^{2+} diet, indicating that CB-D28k is also regulated by Mg^{2+}.

In the kidney, immunoreactivity against PV and CB-D9k is detected in the rat distal convoluted tubule and the latter also in the connecting tubule. The strongest staining localized to the basolateral membranes was used as an argument proposing a role in the regulation of Ca^{2+} transport processes rather than a role as a Ca^{2+} buffer and/or Ca^{2+} shuttle [107, 119]. This is in contrast to the theoretical work describing CB-D9k as a Ca^{2+} buffer/shuttle optimally tuned for transcellular Ca^{2+} transport [120]. Increased transcellular Ca^{2+} transport in a colon cancer cell line (Caco-2) is observed *in vitro* after D3 administration, which leads to an increase in CB-D9k levels hypothesized to cause facilitation of transcellular Ca^{2+} transport [121].

Calbindin-D28k

Structural and general aspects of CB-D28k

CB-D28k has six EF-hand domains, four of which bind Ca^{2+} with medium/high affinity in the intact protein [122]. In all studies EF-hand 2 is considered non-functional, while EF-hand 6 may bind Ca^{2+}, albeit with very low affinity. This, however, was determined not in the intact protein, but using a peptide comprising the sequence of EF-hand domain 6 [123, 124]. In classical terms, the four medium/high affinity sites, sites 1, 3, 4 and 5 ($K_{D,Ca}$ ~500 and 200 nM, respectively, for details, see below; [125]) are considered to be Ca^{2+}-specific sites, although Mg^{2+} binding to the same sites with much lower affinity ($K_{D,Mg}$ ~700 μM) would also allow the classification as Ca^{2+}/ Mg^{2+} mixed sites. Thus, in the presence of physiological Mg^{2+} concentration (0.5–1 mM [34, 35]), the apparent Ca^{2+} affinity is decreased by approximately a factor of 2 and, moreover, cooperativity of Ca^{2+} binding in CB-D28k increases [126]. Compared to PV, the on-rate of Ca^{2+} binding of CB-D28k under physiological conditions inside a cell (k_{on} ~1.1×10^7–8×10^7 $M^{-1}s^{-1}$) is almost one order of magnitude faster (PV: 3×10^6–6×10^6 $M^{-1}s^{-1}$ [20]), in particular it is the faster sites that have lower affinities [125]. Thus, in activated neurons, already the early phase of Ca^{2+} transients are affected by CB-D28k, blunting the peak amplitude of Ca^{2+} transients as has been shown in Purkinje cells of CB-D28k-/- mice [127]. Nonetheless, the time to peak is not significantly affected in the absence of CB-D28k, indicating that the initial $[Ca^{2+}]_i$ rise is essentially governed by the properties of the Ca^{2+} channels, albeit Ca^{2+} binding to CB's fast, medium-affinity sites in WT

Purkinje cells already occurs during the early rising phase as modeled before (Fig. 7D in [70]).

Mobility of CB-D28k and CB-D28k interaction partners

The mobility of CB-D28k inside cells, *i.e.*, in spiny dendrites of cerebellar Purkinje cells, was addressed by FRAP experiments. While the majority of CB-D28k molecules move with a diffusion coefficient of 20 $\mu m^2/s$ [128], approximately twofold slower than PV measured in the identical cellular compartments and, according to the model expectations, in comparison to dextrans of similar molecular weight, an immobile fraction is observed in spines and dendrites, but not in axons of Purkinje cells. The immobilization involving approximately 20 % of CB-D28k molecules in spines and dendrites lasts for several seconds and can be increased by climbing fiber stimulation at either 1 or 20 Hz, in the latter case immobilization is even more enhanced (~70 % higher than in unstimulated cells; [128]). The interacting binding partner in Purkinje cell spines and dendrites is *myo*-inositol monophosphatase (IMPase), a key enzyme of the inositol-1,4,5-triphosphate signaling cascade. *In vitro* CB-D28k associates with IMPase [129] as well as with Ran-binding protein (RanBP) M [130] as evidenced by NMR methods. Additional reported CB-D28k binding partners include caspase-3 [131], 3',5'-cyclic nucleotide phosphodiesterase [132] and plasma membrane ATPase [133]. Recently, the L-type Ca^{2+} channel subunit CANAC1C [134] was identified as a binding partner of CB-D28k, and in the kidney CB-D28k binds to TRPV5 and modulates its activity [135] (see '*Transgenic mice used to study the "Ca^{2+} homeostasome" in renal and intestinal Ca^{2+} regulation*' below). The binding peptide SKSIKNLEP of procaspase-3 is highly similar to the reported IMPase peptide (see below), suggesting that both bind to the same epitope on CB-D28k [136]. These studies together with those on Ca^{2+}-dependent conformational changes indicate that CB-D28k also has characteristics of a Ca^{2+} sensor [126], although the Ca^{2+} dependency of the interaction between CB-D28k and binding partners has not been directly demonstrated yet. The binding sites in CB-D28k interacting with RanBP M have been mapped by NMR and include the N terminus and two regions that exhibit conformational exchange on the NMR timescale (Fig. 2) [130]. NMR interactions with the IMPase peptide SYSSIAKYPSHS yielded essentially identical results, indicating that both IMPase and RanBP M bind to CB-D28k in a similar fashion. In further support of CB-D28k acting as a Ca^{2+}-sensor is the finding that retroviral-mediated overexpression of CB-D28k in hippocampal progenitor cells increases neuronal differentiation and also neurite outgrowth [137]. The same study showed that increased CB-D28k also increases expression of basic helix-loop-helix transcription factors and the phosphorylation of CaM-dependent protein kinase II (CaMKII) and of NeuroD in both fetal and adult hippocampal progenitor cells. Whether the effect is truly specific for CB-D28k or a general Ca^{2+}-buffering effect was not addressed.

NMR structure of CB-D28k

Structural data on CB-D28k have appeared only very recently, despite several labs including the author's own attempting to obtain crystals for the six EF-hand proteins CB-D28k and CR. In 2006, the solution structure of Ca^{2+} -bound rat CB-D28k, the largest structure solved then, was elucidated by NMR [136]. The protein depicted in Figure 2 is made of a single, almost globular (ellipsoid) fold consisting of six distinct EF-hand domains. As explained above, the peptide regions of RanBP M, procaspase-3 and IMPase interact with a surface of CB-D28k consisting primarily of the N-terminal part, the first helix of EF-hand domain 3, the second helix of domain 4 and residues in the linker regions EF2-EF3 and EF4-EF5 of CB [136]. Interestingly, when comparing the residues proposed to either directly bind the target peptides (Ala_2–Asn_7; [130]) or to undergo significant conformational changes [136], the residues show low homology to the closely related CR (Fig. 2), suggesting that CR would likely not bind to the CB-D28k targets, a hypothesis that could be tested experimentally. A brief report on the crystal structure of human CB-D28k has appeared, but no details have been given so far [138].

Functional aspects of CB-D28k

Since its discovery in the 60 s, many roles for CB-D28k have been proposed and include a role in Ca^{2+} resorption in the kidney, modulation of insulin production and secretion in pancreatic β cells [139, 140] and neuroprotection against excitotoxicity. Results on a neuroprotective role are rather inconsistent (*e.g.*, [141–146]; some earlier work is summarized in [64, 77]). The role of CB-D28k in renal Ca^{2+} resorption is addressed below. In 1997, the production of CB-D28k-null mutant mice (systematic name: $Calb1^{tm1Mpin}$; Table 1) was reported; CB-D28k-/- mice manifest no overt phenotype that is related to (a) development, (b) the general morphology of the nervous system or (c) behavior under standard housing conditions [127]. However, the mice show a mild impairment in motor coordination/motor learning [75, 127] that is likely the result of the observed 160-Hz oscillations in the cerebellum [73, 76] (see also section

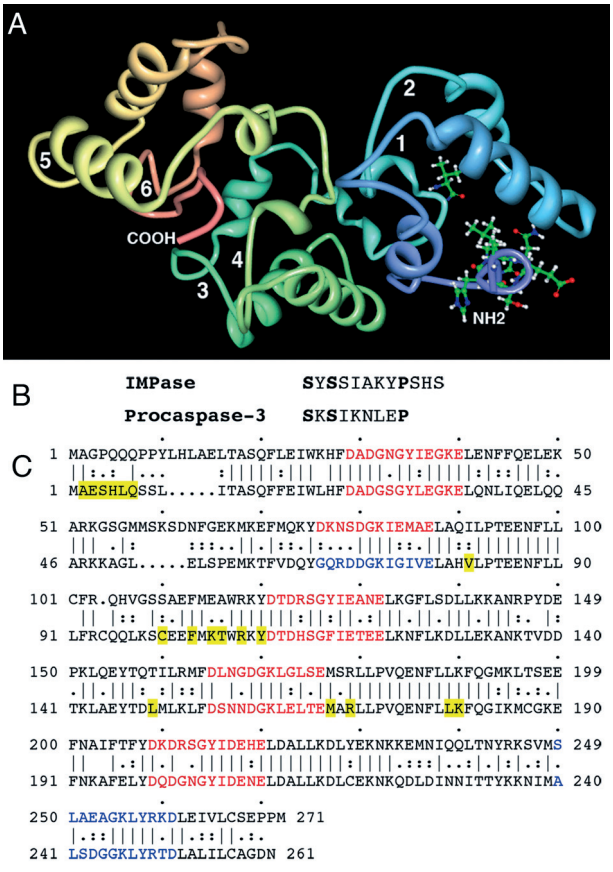

Figure 2. The three-dimensional structure of CB-D28k based on NMR measurements [136]. (*A*) The protein (shown is the backbone) has a relatively compact structure and consists of four functional (1, 3, 4 and 5) and two non-functional (2, 6) EF-hand domains. The Ca^{2+}-binding loops flanked by the two α-helical regions are numbered from 1 to 6. From the N-terminal (NH_2) region (dark blue, EF1) the protein extends to the C terminus (COOH) and changes the color along its way from light blue (EF2), bluish-green (EF3), green (EF4), yellow-orange (EF5) and orange-red (EF6). Side chains are shown for amino acids strongly changing the NMR signal after binding to the interacting peptide IMPase or RanBP M (for details, see text). The most strongly affected residues lie within the most N-terminal region, but the binding interface also includes Val_{90}, the first helix of EF-hand domain 3, the second helix of domain 4 and residues in the linker regions EF2-EF3 and EF4-EF5 of CB-D28k (side chains not shown) [136]. The binding region extends from the N terminus up to approximately the center of the image. The image was generated using PDB ProteinWorkshop 1.50 [228] using the structure of calbindin (CB)-D28k (PDB coordinates 2G9B). (*B*) Sequence comparison of the peptides derived from *myo*-inositol monophosphatase (IMPase) (upper) and procaspases-3 (lower) binding to CB-D28k. (*C*) Amino acids of CB-D28k (lower sequence), whose NMR signals most strongly change after peptide binding (yellow) are generally poorly conserved between human CB-D28k and calretinin (CR) (upper sequence), indicating specificity of ligand binding. The amino acids comprising the functional Ca^{2+}-binding loops, 1–5 in CR and 1, 3, 4 and 5 in CB-D28k, are marked red, the non-functional ones blue.

on *Calretinin* below). The importance of CB-D28k in cerebellar Purkinje cells and cerebellar function is seen in a mouse strain, where the protein is selectively eliminated in Purkinje cells [147]. Both, the motor coordination phenotype and the alterations in Purkinje cell physiology are almost identical to the ones seen in the "global" KO (CB-D28k-/-) mouse strain [148]. It consists of changes in synaptically evoked postsynaptic Ca^{2+} transients, *i.e.*, the amplitude is increased and the fast, but not the slow, $[Ca^{2+}]_i$ decay component has a larger amplitude in CB-D28k-/- than in WT mice [127]. The contribution of CB-D28k in the modulation of Ca^{2+} signals in Purkinje cell dendrites and spines was further determined by comparing Ca^{2+} transients in PV-/- cells with those from PV-/-CB-D28k-/- ones, assuming that the differences in the Ca^{2+} signals are brought about by the absence of CB-D28k [70]. In the first ~100 ms, CB-D28k acts as a Ca^{2+} buffer reducing the peak $[Ca^{2+}]_i$ amplitude to about one half, while from this time on the protein acts as a Ca^{2+} source, slowing the later phase of the $[Ca^{2+}]_i$ decay. Not only the slow buffer PV contributes to the biphasic $[Ca^{2+}]_i$ decay kinetics, but also the high-affinity Ca^{2+}-binding sites of CB-D28k characterized by rather slow kinetics [125] contribute to the biphasic decay. Despite the marked differences in the shape of Ca^{2+} transients, the absence of CB-D28k in Purkinje cells has no effect on the long-term depression (LTD) of Purkinje cell-parallel fiber synaptic transmission [148], suggestive of putative compensation mechanisms. On the other hand elimination of type 1 inositol 1,4,5-triphosphate receptor implicated in the same metabotropic glutamate receptor/IP_3/Ca^{2+} signaling pathway is accompanied with both severe ataxia and impaired LTD [149].

Modulation of synaptic plasticity by CB-D28k

The absence of CB-D28k also affects short-term plasticity evidenced either in cortical multipolar bursting cells (MBC) or at the mossy fiber-CA3 pyramidal cell synapse in the hippocampus [150]. The saturation of mobile, fast, high-affinity cytosolic Ca^{2+} buffers transiently decrease the presynaptic Ca^{2+}-buffering capacity leading to enhanced facilitation [29, 151] and this mechanism is termed "facilitation by buffer saturation". Thus, the elimination of a fast buffer either in CB-D28k-/- neurons or as a consequence of the washout of cytosolic constituents in WT cells *via* the patch pipette increases the amplitude of the first response and subsequently decreases the paired-pulse ratio. The effect of CB-D28k in this process is to cause a decrease in presynaptic $[Ca^{2+}]_i$ and hence the inhibitory post-synaptic-potential during the first response in the paired-pulse protocol. This effect is observed after adding the fast synthetic buffer BAPTA or CB-D28k to the MBC-attached pipette [150]. The modulation of synaptic transmission by the addition of exogenous

buffers such as BAPTA has been described before and was termed pseudofacilitation [152, 153].

A rather similar process also exists in other neurons and was initially observed in tissue obtained from postmortem brains of patients with Ammon's horn sclerosis [154], in an animal model of mesial temporal lobe epilepsy, and in CB-D28k-/- mice [155]. In all three cases, CB-D28k is absent from granule cells of the dentate gyrus. This significantly increases the Ca^{2+}-dependent inactivation of voltage-dependent Ca^{2+} currents (I_{Ca}) and diminishes Ca^{2+} influx during repetitive neuronal firing, an effect that is lost on adding BAPTA or CB-D28k to the pipette. Hence, the loss or down-regulation of CB-D28k may be viewed as a protective or homeostatic mechanism to limit Ca^{2+} influx to increase the resistance against excitotoxicity and to protect the surviving neurons.

The two parameters of a Ca^{2+} buffer, *i.e.*, the Ca^{2+}-binding kinetics together with the mobility define the range of action of a Ca^{2+} ion in the presence of one or several CaBPs, affecting excitability, and also plasticity, not only short-term, but also long-term plasticity. In a model study, the spino-dendritic coupling in Purkinje cells and the role for dendritic Ca^{2+} homeostasis and downstream signaling cascades was investigated using data obtained in PV-/- and CB-D28k-/-PV-/- mice [156]. CB-D28k is the more important "Ca^{2+} transporter" than PV that, by buffered diffusion, also transiently increases $[Ca^{2+}]_i$ in dendritic shafts. These $[Ca^{2+}]_i$ elevations appear sufficient to activate CaM and thus, CaM-dependent processes, representing a novel form of signal integration mediated by the properties of CB-D28k.

Role of CB-D28k in the auditory and visual system

CB-D28k is expressed in specific neurons in the visual and auditory systems, thus the putative role of CB-D28k was studied in CB-D28k-/- mice. CB-D28k is expressed in hair cells of the inner ear, most prominently in the OHC, where concentrations of 160–230 μM were measured in rat neurons [53] and within distinct neurons of the auditory pathway. Surprisingly, no differences either in the auditory brainstem-evoked response, in the distortion-product otoacoustic emissions or in noise-induced trauma that results in hair cell loss were observed when comparing WT with CB-D28k-/- mice [157]. At that time it was not yet known that hair cells also express significant amounts of CR and PV (α PV in both OHC and IHC), β PV most strongly in OHC [53]). Thus, it may well be that the remaining CaBPs compensate for the loss of CB-D28k and these results do not necessarily argue against an essential role for CB-D28k either in hearing or in protecting against moderate noise-induced inner ear traumata. Results obtained in mice without the major CaBPs present (CB-D28k, PV, CR) will hopefully shed more light on that topic (Pangrsic et al., unpublished). Also, the absence of CB-D28k from horizontal cells in the retina of CB-D28k-/- mice has no apparent effect on the histology of the horizontal cell layer, indicating that CB-D28k is not essential for the structural maintenance of the differentiated retina [158], but functional data have not yet been presented.

Transgenic mice used to study the "Ca^{2+} homeostasome" in renal and intestinal Ca^{2+} regulation

The availability of transgenic mouse models has significantly extended our view on physiological Ca^{2+} regulation in the intestine and kidney. Moreover, it has revealed a tight interplay of molecules involved in Ca^{2+} regulation, and this entity has been named the Ca^{2+} signalsome [159] or also Ca^{2+} homeostasome [21]; most often the terms are used in relation to excitable cells such as muscle cells or neurons. The best-studied molecules in the intestinal and renal Ca^{2+} regulation include the main apical Ca^{2+} channel transient receptor potential vanilloid 5 (TRPV5; previously known as ECaC1 [160]) and TRPV6 (previously known as CaT1) in the kidney and intestine, respectively, and the CaBPs (CB-D28k, CB-D9k) and the Na^+/Ca^{2+} exchanger (NCX1) and plasma membrane Ca^{2+}-ATPase (PMCA1b) concentrated in the basolateral membrane. Results from KO mice for CB-D28k, CB-D9k and other molecules involved in the regulation of these are summarized and the available transgenic strains are listed in Table 1. Before discussing specific details, few general conclusions can be drawn: (a) none of the knocked down genes is absolutely essential for Ca^{2+} resorption indicative of complex regulation with built-in redundancy, (b) KO phenotypes under standard diets are surprisingly mild, but become apparent upon experimental manipulation, (c) some counter-intuitive mouse phenotypes can only be explained when compensatory or "homeostatic" mechanisms are considered, and (d) the current data still do not to allow for deducing the "precise" function of the knocked-down proteins.

CB-D28k-/- mice show normal serum values for ionized Ca^{2+}, phosphate, PTH and urine Ca^{2+} excretion (urine Ca^{2+}/creatinine) [161]. Since compensation by CB-D9k was hypothesized to correct for the loss of CB-D28k, and vitamin D receptor (VDR) KO mice, characterized by hypocalcemia, secondary hyperparathyroidism, rickets and osteomalacia, have significantly decreased CB-D9k levels (by 90%), the role of the two CaBPs was investigated in VDR/CB-D28k double-KO mice [161]. Alterations due to changes in the Ca^{2+} regulation (increased urinary

Ca^{2+} excretion, lower bone mineral density) are more pronounced in the double-KO mice compared to mice only deficient in VDR. The phenotype can be partially normalized when mice are fed a high Ca^{2+}, high lactose diet, but skeletal abnormalities persist in the double-KO mice, implicating CB-D28k as also playing an important role in maintaining Ca^{2+} homeostasis. To address the role of renal CB-D28k, double mutants also deficient in TRPV5 (TRPV5-/-) were produced [162]. Hypercalciuria is observed in double-KO mice fed either a 0.02 % or 2 % Ca^{2+} diet, as in TRPV5-/- mice, but not in mice lacking only CB-D28k. In addition, in both strains without TRPV5, an equivalent increase in renal CB-D9k expression as well as an up-regulation of CB-D9k and TRPV6 in the duodenum occurs, resulting in intestinal Ca^{2+} hyperabsorption. None of these compensation mechanisms are induced in CB-D28k-/- mice, indicating a "gatekeeper function" of TRPV5, while the absence of CB-D28k might possibly be compensated by up-regulation of CB-D9k. A tight link between CB-D28k and TRPV5 not only exists at the level of co-localization in the same kidney epithelial cell population, but also at the level of molecular interactions. At low intracellular Ca^{2+}, CB-D28k translocates to the apical plasma membrane and by a direct interaction with TRPV5 modulates its activity [135]. Rapid binding of subplasmalemmal Ca^{2+} by CB-D28k prevents the Ca^{2+}-dependent inactivation of the TRPV5 channels, thus allowing for a larger Ca^{2+} influx. A similar mechanism has already been observed in hippocampal granule cells in CB-D28k-/- mice, albeit only functionally, where the increased Ca^{2+}-dependent inactivation of voltage-dependent Ca^{2+} currents (I_{Ca}) led to a diminished Ca^{2+} influx [163].

The first functional KO for CB-D9k (S100G) was reported in 2006 [164]; in an embryonic stem (ES) cell line, a frameshift deletion in murine S100G was detected and these cells were used to produce transgenic mice. CB-D9k null-mutant mice are indistinguishable from WT controls with respect to reproduction and also have normal serum Ca^{2+} levels, indicating that a functional S100G gene is not required for the most basic physiological functions including reproduction. Furthermore, intestinal Ca^{2+} absorption under normal diet conditions in response to D3 is not impaired, indicating that CB-D9k is not strictly required for vitamin D-induced intestinal Ca^{2+} absorption [165]. Independently, a specifically targeted S100G gene KO was reported in 2007 by Jeung and coworkers [166]. These mice also have no apparent phenotype and the active intestinal Ca^{2+} transport is normal. The authors proposed that homeostatic mechanisms in the intestine, *i.e.*, up-regulation of TRPV6 and PMCA1b during preweaning ,and additional renal homeostatic mechanisms in the adult possibly lead to an almost undetectable phenotype under standard diet conditions. In double mutants additionally deficient for TRPV6, Ca^{2+} serum levels are the same as in single mutant mice (CB-D9k-/-, TRPV6-/-) or control WT mice [167]. In both groups lacking TRPV6, serum PTH levels are increased 1.8-fold, but more importantly, the increase in active intestinal (duodenal) Ca^{2+} transport under low dietary Ca^{2+} conditions is smaller in TRPV6-/- (2.9-fold), and even smaller in the double mutants (2.1-fold) compared to CB-D9k-/- and WT mice: 4.1- and 3.9-fold, respectively. Administration of D3 to vitamin D-deficient mice of all four groups led to a significant increase (40–100 %) in duodenal Ca^{2+} transport. This hints that eliminating the previously thought "essential components" in intestinal absorption (TRPV6 and CB-D9k) only reduces, but not eliminates vitamin D-induced active intestinal Ca^{2+} transport strongly suggestive of additional vitamin D-dependent absorption mechanisms.

The modulation of the Ca^{2+} homeostasome by dietary Ca^{2+} and D3 was also investigated in mice deficient for 25-hydroxyvitamin D3–1α-hydroxylase (1α-OHase-/- mice) [168]. The observed decrease in serum Ca^{2+} levels is the likely result of diminished levels of TRPV5, CB-D9k, CB-D28k and NCX1. Feeding mice with a Ca^{2+}-enriched diet or D3 repletion normalizes levels of proteins involved in Ca^{2+} resorption and also serum Ca^{2+}; yet Ca^{2+} enrichment alone is not sufficient to normalize CB-D9k expression. Nonetheless, serum Ca^{2+} levels are also normal under these conditions, as in the CB-D9k-/- mice, supporting the hypothesis of functional redundancy. In a model of Crohn's disease, TNF(DeltaARE/+) mice are characterized by an approximately 50 % decrease in D3 that accompanies with decreased protein levels of duodenal CB-D9k and renal CB-D28k; at the level of mRNA, TRPV6 and PMCA1b (duodenum) and renal TRPV5 and NCX1 mRNA are also down-regulated [169]. The unchanged serum Ca^{2+} levels in these animals can only be maintained by a Ca^{2+} loss from bone (reduced trabecular and cortical bone thickness and volume), a likely compensation mechanism to cope with the general Ca^{2+} shortage in these mice. Also pharmacological interventions with diuretics (chlorothiazide, furosemide) affect the expression of the above molecules involved in renal Ca^{2+} regulation (details can be found in [112]). Although much has been learned from the various transgenic mouse models, the results indicate that other, yet-undiscovered mechanisms must be present to additionally regulate intestinal and renal Ca^{2+} resorption.

Calretinin

General aspects of CR

CR consists of 269–271 amino acids (depending on the species), organized in six EF-hand domains, five of which are able to bind Ca^{2+} ions [108, 170, 171]. Currently, no structural data (X-ray or NMR) is available for full-length CR, but NMR results were published on the N-terminal 100 amino acids of rat CR consisting of EF-hand domains 1 and 2 [172]. The two domains form a relatively tight structure, while the linker region between domains is exposed to solvent and accessible for proteolytic enzymes. Limited proteolysis studies on the full-length protein and thiol reactivity experiments suggest that the C terminus of CR is in relatively close proximity to site 1 [108]. This is also the case for CB-D28k (Fig. 2), suggesting that the overall structure of the two proteins is likely very similar. The fact that the fluorescence of the hydrophobic probe 2-p-toluidinylnaphtalene-6-sulfonate is markedly enhanced by CR already in the absence of Ca^{2+} and even further increased by Ca^{2+} binding hints that CR might also belong to the "sensor"-type family of CaBPs. This proposition is also based on additional *in vitro* studies on the properties of CR (reviewed in [173]).

Flow dialysis experiments showed that human CR contains four Ca^{2+}-binding sites with positive cooperativity (n_H =1.3) that are half-filled by Ca^{2+} ions at 1.5 μM Ca^{2+} and a fifth site with much lower affinity (intrinsic dissociation constant K'_D of 0.5 mM; [108]). An even higher cooperativity (n_H =1.9) is observed for chick CR [171]. The most detailed *in vitro* study on the binding parameters of CR was carried out by applying the same methodology, *i.e.*, release of caged Ca^{2+} from DM-nitrophen [174], as used before for the determination of the binding properties of CB-D28k [125]. The prior determination of the kinetic properties of DM-nitrophen, *i.e.*, its binding to Ca^{2+} and Mg^{2+} [175] was a requirement for the accurate modeling of CR. Faas and co-workers [174] developed a new mathematical model to determine the dynamic properties of cooperative binding to gain a better understanding of the physiological implications of cooperativity. In line with previous experiments, CR is modeled as a protein with four cooperative binding sites and one independent binding site, and results are summarized in Table 2. In the model, the cooperative pairs of binding sites influence each other in an allosteric manner. Within one pair, each binding site is in a T (tense) state with a low affinity and slow binding rates, if the other binding site is unoccupied, whereas it is in an R (relaxed) state with a high affinity and fast binding rates, if the other binding site is occupied. This causes the association rate of Ca^{2+} with CR to speed up as the free Ca^{2+} concentration increases from cytoplasmic resting conditions (~100 nM) to approximately 1 μM. Thus, the Ca^{2+} -buffering speed of CR strongly depends on the prevailing Ca^{2+} concentration prior to a perturbation and the functional consequences of the unexpected Ca^{2+}-binding properties are discussed below.

Functional aspects of CR

After its initial characterization in 1987 [8], most papers on CR focused on the question where and when the protein is expressed in (a) different species, (b) different tissues, (c) different cell types, sometimes even subcellular compartments, and (d) in certain pathological conditions (*e.g.*, [176]). Results from these earlier studies are, at least in part, summarized in [77, 78, 177]. Indirectly, a protective role against excitotoxicity was inferred from the finding that cortical CR-expressing neurons are more resistant against glutamate toxicity than the general neuron population [178] and that CR-immunoreactive neurons are resistant to β-amyloid toxicity *in vitro* [179], but no experimental proof was presented that CR is directly involved in the protective mechanism. Direct experimental manipulation of CR expression in CR-expressing colon cancer cells revealed that down-regulation by antisense oligos leads to a blockage of the cell cycle and an increase in apoptosis [180]. CR overexpression in PC12 cells provides no protection against Ca^{2+} overload induced by Ca^{2+} ionophore treatment or trophic factor deprivation [181]. Also the presence of CR at an estimated concentration of 1 μM in transfected glioma C6 cells does not significantly affect Ca^{2+} transients induced by ionomycin, ADP or thapsigargin [182]. This is not very surprising based on the later acquired knowledge that CR concentrations within neurons are likely to be in the order of tens of micromolar [53, 183] and that fast buffers mainly affect short-lived Ca^{2+} transients typically seen after AP induction (see below).

The next major step in elucidating the functions of CR was the generation of CR-null-mutant mice (CR-/-; systematic name: $Calb2^{tm1Map}$; Table 1) in 1997 [184], where impaired long-term potentiation (LTP) in the hippocampus was the first reported alteration. Basal synaptic transmission between the perforant pathway and granule cells, and also at the Schaffer commissural input to CA1 pyramidal neurons is unchanged. Yet tetanic stimulation of the perforant pathway increases the excitatory drive from CR-deficient mossy cells onto hilar interneurons, and the excess of GABA release onto dentate granule cells is thought to cause the inhibition of LTP induction. This hypothesis is based on the fact that LTP impairment can be prevented by the GABA blocker bicuculline. Unlike

most other CaBP KO mice, where the heterozygous animals rarely show a phenotype, impaired LTP is also seen in CR+/- mice indicating that half of the CR expression levels compared to WT control mice is not sufficient to sustain normal LTP [185]. The rather uniform expression of CR in cerebellar granule cells and the stereotypic organization of the cerebellum have made this the prime site for the *in vivo* investigation of the physiological function of CR. Granule cells provide the major excitatory input onto Purkinje cells *via* the parallel fibers, thus allowing the role of CR in presynaptic terminals to be addressed, whereas stimulation of mossy fibers contacting the soma of granule cells is expected to yield information on the role of postsynaptic CR. Impairment of motor coordination in CR-/- mice is linked to altered Ca^{2+} homeostasis in Purkinje cells, indirectly supported by the increased Ca^{2+} saturation of CB-D28k in these cells [186]. As in CB-D28k-/- and PV-/- mice, the firing properties of Purkinje cells are altered in alert CR-/- mice. The most notable changes include an increase in the simple spike firing rate, a shortening of the complex spike duration, and a shortening of the spike pause [186]. At the network level, these altered firing properties likely lead to the emergence of 160-Hz oscillations [73], not observed in WT mice. The similarity of the oscillations in mice deficient for either PV, CB-D28k or CR indicates an effect at the system level. Thus, pharmacological blocking of (a) gap junctions between interneurons, (b) the *N*-methyl-D-aspartate receptors, or (c) the $GABA_A$ receptors by gabazine reversibly attenuates these oscillations. This indicates that oscillations emerge *via* a mechanism that synchronizes assemblies of Purkinje cells (mediated by parallel fiber excitation) and the network of chemically coupled molecular layer interneurons (stellate/basket cells), although the putative involvement of networking by recurrent Purkinje cell collaterals was recently emphasized [187]. Granule cells of CR-/- mice show faster action potentials and, under conditions generating repetitive spike discharges, show enhanced frequency increase with injected currents [183]. The effect can be reversed in the presence of the fast buffer BAPTA (150 μM) in the recording pipette, arguing that CR under these conditions functions as a "fast" Ca^{2+} buffer, but this is not the only mode of how CR might work inside cells (see below). Further support that the CR deficiency in granule cells is responsible for the observed 160-Hz oscillations comes from the findings on CR "rescue" mice, where CR is selectively re-expressed in granule cells of otherwise CR-deficient mice [188] using the $GABA_A$ receptor α6 promoter [189] to drive CR expression selectively in this neuron population. In alert "rescue" mice, normal granule cell excitability and Purkinje cell firing is restored resulting in neither 160-Hz oscillations nor impairment in motor coordination. Thus, subtle disturbances in the modulation of Ca^{2+} transients in the subpopulation of neurons expressing CR [73], CB-D28k or PV [76] in the cerebellum impairs cerebellar functions, indicating that Ca^{2+} homeostasis is crucial for the coding and storage of information in the cerebellum.

CR may function as a "fast" and as a "slow" buffer

That CR also works as a "slow" Ca^{2+} buffer was gleaned from experiments with *Xenopus* oocytes. Direct injection or cDNA-mediated overexpression of the "slow" buffer PV induces elementary Ca^{2+} release events by Ca^{2+}-induced Ca^{2+} release (CICR) resulting in Ca^{2+} puffs, which are elicited from discrete clusters of inositol 1,4,5 triphosphate receptors (IP_3R) at low concentrations of IP_3 [190]. Similar Ca^{2+} puff activity also occurs after EGTA injection, but not in the presence of the fast buffer CB-D28k. In general, fast buffers such as BAPTA blunt the amplitudes of Ca^{2+} responses and at the same time promote the "globalization" of spatially uniform Ca^{2+} signals [191]. Thus, the distinct kinetic properties of Ca^{2+} buffers strongly influence the time course and spatial distribution of IP_3-evoked Ca^{2+} signals. An unexpected finding was observed with CR, based on previous experimental results showing that CR behaves like the fast buffer BAPTA in modifying presynaptic Ca^{2+} signaling in frog saccular hair cells [192]. In *Xenopus* oocytes at low IP_3 release conditions resulting in only small Ca^{2+} transients, CR induces Ca^{2+} puffs, which are never observed with BAPTA, but are typical for "slow" Ca^{2+} buffers. This dual behavior results from the particular Ca^{2+}-binding properties of CR, in particular the strong cooperativity between the paired binding sites (1–2 and 3–4) discussed above. Small Ca^{2+} elevations will only activate the two cooperative binding sites in the T state that are characterized by a rather low affinity (28 μM) and a slow on-rate ($1.8\times10^6\ M^{-1}s^{-1}$) [174]. The effects of CR on a train of ten dendritic Ca^{2+} transients were modeled and compared to BAPTA (fast) and EGTA (slow) (Fig. 3; kindly provided by G. Faas, UCLA, for details on the model, see legend). In the model, Ca^{2+} channels open for 10 ms at 50-ms intervals (20 Hz). From a resting $[Ca^{2+}]_i$ of 100 nM, in the absence of buffers (dashed line) the peak maximum reaches ~10 μM. By adding 30 μM CR, *i.e.*, 150 μM of Ca^{2+}-binding sites, the initial peak amplitude is reduced to ~3 μM (black line), but due to continuous sequestering and releasing Ca^{2+} during the following series, $[Ca^{2+}]_i$ does not return to the initial level of 100 nM, but slowly rises to ~0.8–1 μM (inset). When $[Ca^{2+}]_i$ is still relatively low before the next Ca^{2+} influx (<500 nM, area A), CR

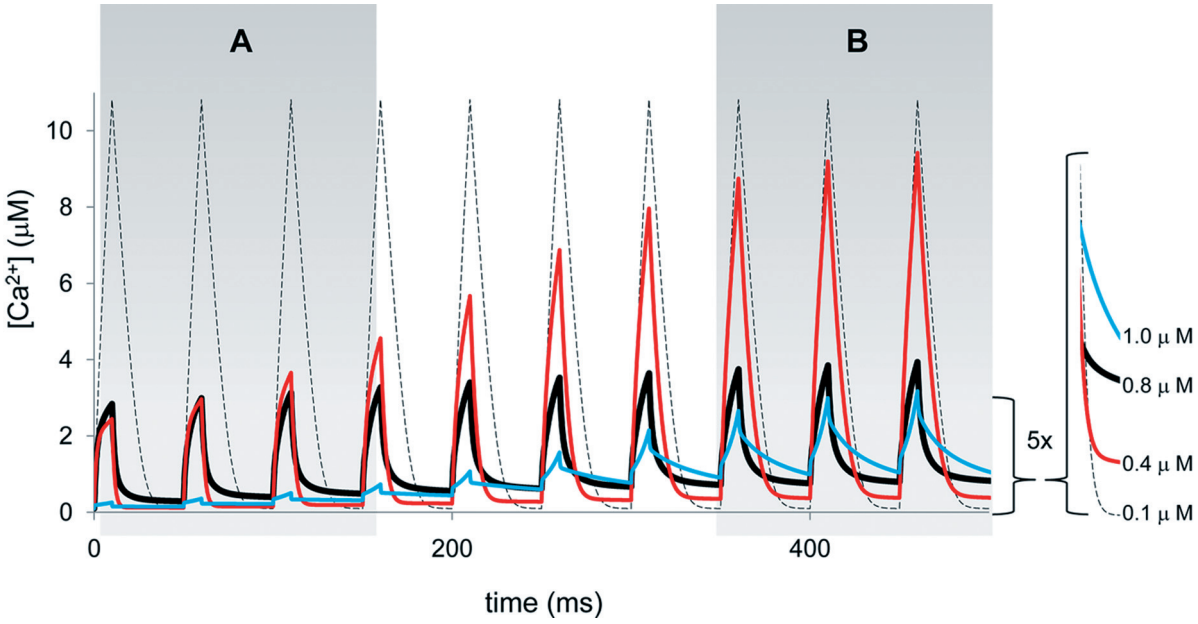

Figure 3. Effect of Ca^{2+} buffers on dendritic Ca^{2+} signals (simulations with Berkeley Madonna using a single compartment model; for additional details, see [174]). In a cylinder-shaped dendritic compartment (r =1 μm, l =10 μm), Ca^{2+} channels open ten times for 10 ms every 50 ms (20 Hz). The current of 10 pA corresponds to opening of ~3–5 channels, depending on the channel type and extracellular $[Ca^{2+}]$. The membrane contains Ca^{2+} pumps (K_m =3 μM, v_{max}=50 pmol cm^{-2} s^{-1}) [70, 229] that maintain $[Ca^{2+}]_i$ at 100 nM. In the absence of buffers, the peak amplitude is ~10 μM (dashed line) and drops to 100 nM between transients. Addition of CR (30 μM, corresponding to 150 μM Ca^{2+}-binding sites, black line) reduces the amplitude to ~3 μM during the first peak with little variation during consecutive transients. The effect of equivalent amounts (150 μM) of EGTA (red line, K_D 70 nM [125], k_{on} 10^7 M^{-1} s^{-1}) and BAPTA (blue line, K_D 160 nM, k_{on} 2×10^8 M^{-1} s^{-1}) on the shape of Ca^{2+} transients is quite different. Although early transients (area A) look similar in the presence of CR and EGTA, later on with EGTA the amplitude starts to increase (area B). BAPTA almost completely abrogates the peak amplitude in area A and only in the last transients of the train, the Ca^{2+} influx exceeds BAPTA's buffering capacity allowing amplitudes to reaching similar values as in the case of CR (area B). The late phase of the $[Ca^{2+}]_i$ decay after the tenth transient is shown at higher magnification in the inset reporting the residual Ca^{2+} in the presence of the three buffers compared to the situation pertaining in the absence of added buffers. As a result of the non-linear binding properties of CR [174], the amplitudes in the presence of CR remain almost constant throughout the 10 Ca^{2+} transients (for mechanistic details, see section *CR may function as a "fast" and as a "slow" buffer*).

acts as a slow buffer comparable to EGTA (150 μM, red line). More unoccupied Ca^{2+}-binding sites of CR are in the fast R state at the end of the train, when the minimal Ca^{2+} concentration is >700 nM before the next Ca^{2+} pulse (area B). This leads to a more BAPTA-like behavior (blue line) of CR. Thus, the non-linear property of CR causes the shapes of individual transients to remaining practically the same throughout the series (peak maximum ~3 μM), in contrast to the effects induced by either EGTA or BAPTA. The slow buffer EGTA is responsible for the fast initial decay in $[Ca^{2+}]_i$ during the first transient, but the accumulation of Ca^{2+}-bound EGTA ("buffer saturation") leads to a reduced buffering capacity later on, resulting in higher peak amplitudes late in the series (red trace in area B). On the other hand, BAPTA's fast binding kinetics almost completely abolish the Ca^{2+} elevation during the first Ca^{2+} influx and only as the buffering capacity decreases due to BAPTA getting Ca^{2+}-loaded, does the peak amplitude reach values similar to those in the presence of CR (compare blue and black traces in area B). However, typically for a fast buffer, BAPTA considerably slows down the $[Ca^{2+}]_i$ decay by acting as a Ca^{2+} source, a concept initially elucidated in the early 90 s [193–195].

Regulation of CR expression

Very little is known about the physiological regulation of CR expression. In several reports altered expression due to various manipulations have been reported and include down- or up-regulation of CR [196–201]. In the mouse CR gene (CALB2), upstream promoter and enhancer elements including TATA and CAAT boxes show considerable sequence homology to human (*CALB2*) upstream elements [202]. A minimal element ending at –95 bp upstream of the transcription start site confers neuron specificity and the rat –115/–71 CALB2 promoter region contains a binding site for a factor present in brain nuclear extracts (*e.g.*, from cerebellar granule neurons) [203]. This AP2-like element located between –90 and –80 bp appears essential for the neuron-specific activity of the CALB2 promoter. In contrast, this element appears to be non-functional in CR-expressing colon cancer and mesothelioma cells, indicating that CR expression

in neurons and cancer cells is regulated *via* different mechanisms [204]. Specifically in colon cancer cells, addition of butyrate, an enhancer of differentiation, down-regulates CR expression [200]. In several colon cancer cell lines and primary colon tumor tissue, two additional CR transcripts coding for truncated versions of CR are present [205]. The deletion of exons 8 and 9 or of exon 8 only of the human *CALB2* mRNA, leads to a frame shift and premature stop codons, resulting in proteins named CR-22k (192 amino acids, accession no. NP_009019) and CR-20k (179 amino acids, accession no._NP_009018), respectively. So far, these splice variants have only been detected in transformed cells derived from colon [206] or mesothelioma tissue [207], and little is known about the regulation of these transcripts. Nonetheless, the aberrant CR expression is most helpful in identifying mesotheliomas, a tumor of the serosal lining of the body cavities that is often difficult to differentiate from lung carcinomas [208, 209], for example.

During development, CR expression and also intracellular localization are regulated. In brainstem auditory neurons in the chick nucleus magnocellularis, CR immunoreactivity changes from being diffusely dispersed throughout the cytoplasm to being highly concentrated beneath the plasma membrane [210]. This change coincides with the onset of spontaneous activity, synaptic transmission, and synapse refinement in nucleus magnocellularis. It was hypothesized that localization of CR beneath the plasma membrane is an adaptation to spatially restrict the Ca^{2+} influxes (see also next section).

The intracellular Ca^{2+} homeostasome

To use variations in $[Ca^{2+}]_i$ as an intracellular signal, cells must have a finely tunable system regulating $[Ca^{2+}]_i$ most accurately in time and space. An increase in $[Ca^{2+}]_i$ may be brought about by opening of Ca^{2+} channels in the plasma membrane or by a release of Ca^{2+} from internal stores, most importantly from the endoplasmic reticulum (ER). In the cytosol the signal is then modulated by immobile or mobile intracellular Ca^{2+} buffers, in particular CaBPs, and at the end the initial situation is restored by either Ca^{2+} extrusion by plasma membrane Ca^{2+} pumps (PMCA), the Na^+/Ca^{2+} exchanger (NCX) or by uptake into organelles including the ER, mitochondria and possibly also peroxisomes [211]. How does a particular cell "know" how many and which type of the different components of the Ca^{2+} homeostasome are necessary, and how does a cell cope when one or several of these components are missing (*e.g.*, by targeted ablation) or functionally compromised (*e.g.*, in genetic diseases)? It is clear that Ca^{2+} itself is an important regulator of gene expression as evidenced for example in cultured cerebellar granule cells, where neuronal survival is dependent on Ca^{2+} influx induced by membrane depolarization. This leads to the up-regulation of IP_3R and PMCAs, and in parallel, to the down-regulation of one splicing variant of the isoform PMCA4 and one of the Na^+/Ca^{2+} exchangers of the plasma membrane (NCX2) [212]. Thus, a cell has an extensive "Ca^{2+}-signaling toolkit" to precisely shape the Ca^{2+} signaling system also involved in controlling the expression of its own components (for a review, see [159]).

Findings on the Ca^{2+} homeostasome where CaBPs are involved are briefly summarized here. In essentially all reports on CaBP KO mice, the absence of a particular CaBP is not compensated by another EF-hand family member normally not expressed in this cell type, *e.g.*, the subset of PV-immunoreactive (-ir) interneurons in PV-/- mice do neither express CB-D28k, CB-D9k nor CR [72]; correspondingly, the same holds true for the CR-ir or the CB-D28k-ir neurons. This suggests that neurons once committed to express a particular CaBP, are either incapable of turning on the expression of another EF-hand family member with "similar" Ca^{2+}-binding properties or that the distinct properties (affinities, kinetics, mobility) of any other CaBP would not suffice to restore "normal" Ca^{2+} homeostasis [64]. Homeostatic mechanisms observed in the brain of CaBP-KO mice include alterations in the spine morphology (increased length and volume) of Purkinje cells selectively in CB-D28k-/- mice, but not in PV-/- animals [213]. Yet, in the soma of PV-/- Purkinje cells, the volume of mitochondria, organelles involved in Ca^{2+} sequestration and acting as a transient Ca^{2+} store [214] is selectively increased by about 40 % in a narrow zone underneath the plasma membrane, while the density of perinuclear mitochondria is unchanged [215]. At the same time the subplasmalemmal ER compartment is also decreased. All these alterations are not present in CB-D28k-/- Purkinje cells. The inverse relationship between mitochondrial volume and PV expression is also seen in fast-twitch muscle fibers [216] and, interestingly, the mechanism also functions the other way round: ectopic expression of PV in striatal neurons normally not expressing PV decreases the mitochondrial volume by almost 50 % [217], which accounts for the heightened excitotoxic injury provoked by a local injection of ibotenic acid into this transgenic mouse line named Thy-PV mice [218]. Adaptive changes involving CaBPs are also seen in Purkinje cells of leaner [tg(la)] mice characterized by a mutation in the voltage-activated Ca^{2+} channel α(1A) subunit, the pore-forming subunit of P/Q-type

Ca^{2+} channels. The severely reduced Ca^{2+} channel function is "compensated" by a diminished Ca^{2+} buffering/uptake capacity due to decreased Ca^{2+} uptake by the ER and a reduction in PV and CB-D28k expression ([219], for a review, see [220]). Such homeostatic mechanisms involving Ca^{2+} channels and Ca^{2+} buffering are also functional during ageing as observed in basal forebrain neurons [221]. CaBPs also directly modulate the activity of Ca^{2+} channels, including the N-, L- and P/Q-type Ca^{2+} channels. They are involved in both Ca^{2+}-dependent inactivation and facilitation, and the best-studied example is CaM modulating L-type Ca^{2+} channels [222] as well as P/Q-type channels [223]. Both PV and CB-D28k play a role in modulating Ca^{2+}-dependent inactivation, but not facilitation [224] and, interestingly, the two physiological Ca^{2+} buffers affect P/Q-type channel function differently from the synthetic buffers EGTA and BAPTA, often presumed to substitute for "real" CaBPs. The Ca^{2+}-dependent inactivation of P/Q-type channel is assumed to depend on Ca^{2+} microdomains surrounding the Ca^{2+} channels in the plasma membrane and these microdomains are likely to be affected differently by the various Ca^{2+} buffers. This in turn specifically affect the inactivation properties of the Ca^{2+} channels. Alterations in Ca^{2+} extrusion systems by plasma membrane ATPases (PMCA) also modulate the Ca^{2+} homeostasome. A mutation in PMCA2 expressed at particularly high levels in Purkinje neurons is correlated with reduced Ca^{2+} influx due to the down-regulation of voltage-gated Ca^{2+} channels [225]. In PMCA2-/- mice exhibiting ataxia, expression levels of metabotropic glutamate receptor 1 and of inositol 1,4,5-triphosphate receptor type 1 responsible for the Ca^{2+} release from ER stores are down-regulated [226]. In Purkinje cells from CB-D28k-/-PV-/- mice, an increase in Ca^{2+} extrusion mechanisms was postulated, since the decay of dendritic Ca^{2+} signals could only be accurately fitted when using a twofold higher extrusion rate compared to the rates sufficient to model the transients in PV-/- and WT Purkinje cells [70]. Yet the molecular identity (PMCA, NCX, intracellular stores) leading to the increased $[Ca^{2+}]_i$ decay was not investigated in this study.

Conclusions

Studies on the various CaBP-KO mice have revealed that each Ca^{2+} buffer/sensor has distinct functions, which agree with its specific Ca^{2+}-buffering properties. Ablation of a CaBP does not induce the apparently obvious compensatory mechanism, *i.e.*, the up-regulation of a CaBP with properties most closely resembling the eliminated one, but leads to very specific adaptations at the level of other components of the Ca^{2+}-signaling toolkit and morphological changes. In the brain or in the systems involved in Ca^{2+} resorption (intestine, kidney), the adaptive changes are not limited to the population of cells from which a CaBP has been removed, but includes changes in other cell populations functionally connected to the altered (impaired) ones. Thus, CaBP-deficient cells make use of the components of the Ca^{2+}-signaling toolkit [159] to attempt to restore the situation pertaining in unaffected cells; yet the Ca^{2+} homeostasome is even more far reaching, also remodeling Ca^{2+}-signaling components in cells not directly affected by the absence of the ablated CaBP.

Acknowledgements. The modeling on the role of CR shown in Figure 3 was kindly provided by G. Faas, UCLA and is highly appreciated. I would like to thank the following colleagues for helpful comments on the manuscript: Serge Schiffman, Bruxelles; Hartmut Schmidt, Leipzig; Johannes Loffing, Zurich; Joost Hoenderop, Nijmegen; and from Fribourg: Thomas Henzi, Sylvie Ducreux and Patrick Gregory. Evidently the review represents to some extent the author's preferences, thus I apologize for not having cited each important contribution on the role of CaBPs; size restriction did not allow reviewing all the vast literature that has been published within the last 10 years.

1 Henrotte, J. G. (1952) A crystalline constituent from myogen of carp muscles. Nature 169, 968–969
2 Kretsinger, R. H. and Nockolds, C. E. (1973) Carp muscle calcium-binding protein. II. Structure determination and general description. J. Biol. Chem. 248, 3313–3326
3 Taylor, A. N. and Wasserman, R. H. (1967) Vitamin D3-induced calcium-binding protein: Partial purification, electrophoretic visualization, and tissue distribution. Arch. Biochem. Biophys. 119, 536–540
4 Kallfelz, F. A., Taylor, A. N. and Wasserman, R. H. (1967) Vitamin D-induced calcium binding factor in rat intestinal mucosa. Proc. Soc. Exp. Biol. Med. 125, 54–58
5 Kawasaki, H., Nakayama, S. and Kretsinger, R. H. (1998) Classification and evolution of EF-hand proteins. Biometals 11, 277–295
6 Marenholz, I., Heizmann, C. W. and Fritz, G. (2004) S100 proteins in mouse and man: From evolution to function and pathology (including an update of the nomenclature). Biochem. Biophys. Res. Commun. 322, 1111–1122
7 Pochet, R., Parmentier, M., Lawson, D. E. and Pasteels, J. L. (1985) Rat brain synthesizes two 'vitamin D-dependent' calcium-binding proteins. Brain Res. 345, 251–256
8 Rogers, J. H. (1987) Calretinin: A gene for a novel calcium-binding protein expressed principally in neurons. J. Cell Biol. 105, 1343–1353
9 Cheung, W. Y., Lynch, T. J. and Wallace, R. W. (1978) An endogenous Ca^{2+}-dependent activator protein of brain adenylate cyclase and cyclic neucleotide phosphodiesterase. Adv. Cyclic Nucleotide Res. 9, 233–251
10 Kretsinger, R. H. (1980) Structure and evolution of calcium-modulated proteins. CRC Crit. Rev. Biochem. 8, 119–174
11 Lander, E. S., Linton, L. M., Birren, B., Nusbaum, C., Zody, M. C., Baldwin, J., Devon, K., Dewar, K., Doyle, M., FitzHugh, W., Funke, R., Gage, D. et al. (2001) Initial sequencing and analysis of the human genome. Nature 409, 860–921

12 Carafoli, E., Santella, L., Branca, D. and Brini, M. (2001) Generation, control, and processing of cellular calcium signals. Crit. Rev. Biochem. Mol. Biol. 36, 107–260
13 Maki, M., Kitaura, Y., Satoh, H., Ohkouchi, S. and Shibata, H. (2002) Structures, functions and molecular evolution of the penta-EF-hand Ca^{2+}-binding proteins. Biochim. Biophys. Acta 1600, 51–60
14 Ikura, M. (1996) Calcium binding and conformational response in EF-hand proteins. Trends Biochem. Sci. 1, 14–17
15 Nelson, M. R. and Chazin, W. J. (1998) Structures of EF-hand Ca^{2+}-binding proteins: Diversity in the organization, packing and response to Ca^{2+} binding. Biometals 11, 297–318
16 Vetter, S. W. and Leclerc, E. (2003) Novel aspects of calmodulin target recognition and activation. Eur. J. Biochem. 270, 404–414
17 Ikura, M. and Ames, J. B. (2006) Genetic polymorphism and protein conformational plasticity in the calmodulin superfamily: Two ways to promote multifunctionality. Proc. Natl. Acad. Sci. USA 103, 1159–1164
18 Baldellon, C., Alattia, J. R., Strub, M. P., Pauls, T., Berchtold, M. W., Cave, A. and Padilla, A. (1998) N-15 NMR relaxation studies of calcium-loaded parvalbumin show tight dynamics compared to those of other EF-hand proteins. Biochemistry 37, 9964–9975
19 Augustine, G. J., Santamaria, F. and Tanaka, K. (2003) Local calcium signaling in neurons. Neuron 40, 331–346
20 Schwaller, B. (2003) Ca^{2+}-Buffers. In: Handbook of Cell Signaling, vol. 2, pp. 67–71, Bradshaw, R. A. and Dennis, E. A. (eds.), Academic Press, Oxford
21 Schwaller, B. (2007) Emerging functions of the "Ca^{2+} buffers" parvalbumin, calbindin D-28k and calretinin in the brain. In: Handbook of Neurochemistry and Molecular Neurobiology. Neural Protein Metabolism and Function, vol. 7, pp. 197–222, Lajtha, A. and Banik, N. (eds.), Springer, New York
22 Niggli, E. and Shirokova, N. (2007) A guide to sparkology: The taxonomy of elementary cellular Ca^{2+} signaling events. Cell Calcium 42, 379–387
23 Braunewell, K. H. and Gundelfinger, E. D. (1999) Intracellular neuronal calcium sensor proteins: A family of EF-hand calcium-binding proteins in search of a function. Cell. Tissue Res. 295, 1–12
24 Burgoyne, R. D. and Weiss, J. L. (2001) The neuronal calcium sensor family of Ca^{2+}-binding proteins. Biochem. J. 353, 1–12
25 Celio, M. (1996) Guidebook to the Calcium-Binding Proteins. Celio, M., Pauls, T. and Schwaller, B. (eds.). Oxford University Press, Oxford
26 Kawasaki, H. and Kretsinger, R. H. (1994) Calcium-binding proteins 1: EF-hands. Protein Profile 1, 343–517
27 Gomez, J., Neco, P., DiFranco, M. and Vergara, J. L. (2006) Calcium release domains in mammalian skeletal muscle studied with two-photon imaging and spot detection techniques. J. Gen. Physiol. 127, 623–637
28 Neher, E. and Augustine, G. J. (1992) Calcium gradients and buffers in bovine chromaffin cells. J. Physiol. 450, 273–301
29 Neher, E. (1998) Usefulness and limitations of linear approximations to the understanding of Ca^{2+} signals. Cell Calcium 24, 345–357
30 Lips, M. B. and Keller, B. U. (1998) Endogenous calcium buffering in motoneurones of the nucleus hypoglossus from mouse. J. Physiol. 511, 105–117
31 Lee, S. H., Rosenmund, C., Schwaller, B. and Neher, E. (2000) Differences in Ca^{2+} buffering properties between excitatory and inhibitory hippocampal neurons from the rat. J. Physiol. 525, 405–418
32 Fierro, L. and Llano, I. (1996) High endogenous calcium buffering in Purkinje cells from rat cerebellar slices. J. Physiol. 496, 617–625
33 Cox, J. A., Durussel, I., Scott, D. J. and Berchtold, M. W. (1999) Remodeling of the AB site of rat parvalbumin and oncomodulin into a canonical EF-hand. Eur. J. Biochem. 264, 790–799
34 Li-Smerin, Y., Levitan, E. S. and Johnson, J. W. (2001) Free intracellular Mg^{2+} concentration and inhibition of NMDA responses in cultured rat neurons. J. Physiol. 533, 729–743
35 Watanabe, M. and Konishi, M. (2001) Intracellular calibration of the fluorescent Mg^{2+} indicator furaptra in rat ventricular myocytes. Pflugers Arch. 442, 35–40
36 Swain, A. L., Kretsinger, R. H. and Amma, E. L. (1989) Restrained least squares refinement of native (calcium) and cadmium-substituted carp parvalbumin using X-ray crystallographic data at 1.6-Å resolution. J. Biol. Chem. 264, 16620–16628
37 Babini, E., Bertini, I., Capozzi, F., Del Bianco, C., Hollender, D., Kiss, T., Luchinat, C. and Quattrone, A. (2004) Solution structure of human beta-parvalbumin and structural comparison with its paralog alpha-parvalbumin and with their rat orthologs. Biochemistry 43, 16076–16085
38 Henzl, M. T. and Tanner, J. J. (2008) Solution structure of Ca^{2+}-free rat alpha-parvalbumin. Protein Sci. 17, 431–438
39 Henzl, M. T. and Tanner, J. J. (2007) Solution structure of Ca^{2+}-free rat beta-parvalbumin (oncomodulin). Protein Sci. 16, 1914–1926
40 Cox, J. A., Milos, M. and MacManus, J. P. (1990) Calcium- and magnesium-binding properties of oncomodulin. Direct binding studies and microcalorimetry. J. Biol. Chem. 265, 6633–6637
41 Pechere, J. F., Capony, J. P. and Ryden, L. (1971) The primary structure of the major parvalbumin from hake muscle. Isolation and general properties of the protein. Eur. J. Biochem. 23, 421–428
42 Feher, J. J. (1984) Measurement of facilitated calcium diffusion by a soluble calcium-binding protein. Biochim. Biophys. Acta 773, 91–98
43 Maughan, D. W. and Godt, R. E. (1999) Parvalbumin concentration and diffusion coefficient in frog myoplasm. J. Muscle Res. Cell. Motil. 20, 199–209
44 Schmidt, H., Brown, E. B., Schwaller, B. and Eilers, J. (2003) Diffusional mobility of parvalbumin in spiny dendrites of cerebellar purkinje neurons quantified by fluorescence recovery after photobleaching. Biophys. J. 84, 2599–2608
45 Schmidt, H., Arendt, O., Brown, E. B., Schwaller, B. and Eilers, J. (2007) Parvalbumin is freely mobile in axons, somata and nuclei of cerebellar Purkinje neurones. J. Neurochem. 100, 727–735
46 MacManus, J. P., Whitfield, J. F., Boynton, A. L., Durkin, J. P. and Swierenga, S. H. (1982) Oncomodulin – A widely distributed, tumour-specific, calcium-binding protein. Oncodev. Biol. Med. 3, 79–90
47 Brewer, L. M. and MacManus, J. P. (1987) Detection of oncomodulin, an oncodevelopmental protein in human placenta and choriocarcinoma cell lines. Placenta 8, 351–363
48 Pace, J. L., Barger, B. O., Dawe, D. L. and Ragland, W. L. (1978) Specific antigens of chicken thymus. Eur. J. Immunol. 8, 671–678
49 Murthy, K. K., Odend'hal, S. and Ragland, W. L. (1984) Demonstration of T lymphocytes in the bursa of Fabricius of the chicken following cyclophosphamide treatment. Dev. Comp. Immunol. 8, 213–218
50 Murthy, K. K. and Ragland, W. L. (1984) Immunomodulation by thymic hormones: Studies with an avian thymic hormone. Prog. Clin. Biol. Res. 161, 481–491
51 Thalmann, I., Shibasaki, O., Comegys, T. H., Henzl, M. T., Senarita, M. and Thalmann, R. (1995) Detection of a beta-parvalbumin isoform in the mammalian inner ear. Biochem. Biophys. Res. Commun. 215, 142–147
52 Yang, D., Thalmann, I., Thalmann, R. and Simmons, D. D. (2004) Expression of alpha and beta parvalbumin is differentially regulated in the rat organ of corti during development. J. Neurobiol. 58, 479–492
53 Hackney, C. M., Mahendrasingam, S., Penn, A. and Fettiplace, R. (2005) The concentrations of calcium buffering proteins in mammalian cochlear hair cells. J. Neurosci. 25, 7867–7875

54 Moser, T., Brandt, A. and Lysakowski, A. (2006) Hair cell ribbon synapses. Cell. Tissue Res. 326, 347–359

55 Durussel, I., Pauls, T. L., Cox, J. A. and Berchtold, M. W. (1996) Chimeras of parvalbumin and oncomodulin involving exchange of the complete CD site show that the Ca^{2+}/Mg^{2+} specificity is an intrinsic property of the site. Eur. J. Biochem. 242, 256–263

56 Pauls, T. L., Durussel, I., Clark, I. D., Szabo, A. G., Berchtold, M. W. and Cox, J. A. (1996) Site-specific replacement of amino acid residues in the CD site of rat parvalbumin changes the metal specificity of this Ca^{2+}/Mg^{2+}-mixed site toward a Ca^{2+}-specific site. Eur. J. Biochem. 242, 249–255

57 Hou, T.-T., Johnson, J. D. and Rall, J. A. (1992) Effect of temperature on relaxation rate and Ca^{2+}, Mg^{2+} dissociation rates from parvalbumin of frog muscle fibres. J. Physiol. 449, 399–410

58 Jiang, Y., Johnson, J. D. and Rall, J. A. (1996) Parvalbumin relaxes frog skeletal muscle when sarcoplasmic reticulum Ca^{2+}-ATPase is inhibited. Am. J. Physiol. 270, C411-C417

59 Rall, J. A. (1996) Role of parvalbumin in skeletal muscle relaxation. Am. J. Physiol. 270, C411-C417

60 Muntener, M., Kaser, L., Weber, J. and Berchtold, M. W. (1995) Increase of skeletal muscle relaxation speed by direct injection of parvalbumin cDNA. Proc. Natl. Acad. Sci. USA 92, 6504–6508

61 Schwaller, B., Dick, J., Dhoot, G., Carroll, S., Vrbova, G., Nicotera, P., Pette, D., Wyss, A., Bluethmann, H., Hunziker, W. and Celio, M. R. (1999) Prolonged contraction-relaxation cycle of fast-twitch muscles in parvalbumin knockout mice. Am. J. Physiol. 276, C395–403

62 Raymackers, J. M., Gailly, P., Schoor, M. C., Pette, D., Schwaller, B., Hunziker, W., Celio, M. R. and Gillis, J. M. (2000) Tetanus relaxation of fast skeletal muscles of the mouse made parvalbumin deficient by gene inactivation. J. Physiol. 527, 355–364

63 Lee, S. H., Schwaller, B. and Neher, E. (2000) Kinetics of Ca^{2+} binding to parvalbumin in bovine chromaffin cells: Implications for $[Ca^{2+}]$ transients of neuronal dendrites. J. Physiol. 525, 419–432

64 Schwaller, B., Meyer, M. and Schiffmann, S. (2002) 'New' functions for 'old' proteins: The role of the calcium-binding proteins calbindin D-28k, calretinin and parvalbumin, in cerebellar physiology. Studies with knockout mice. Cerebellum 1, 241–258

65 Caillard, O., Moreno, H., Schwaller, B., Llano, I., Celio, M. R. and Marty, A. (2000) Role of the calcium-binding protein parvalbumin in short-term synaptic plasticity. Proc. Natl. Acad. Sci. USA 97, 13372–13377

66 Collin, T., Chat, M., Lucas, M. G., Moreno, H., Racay, P., Schwaller, B., Marty, A. and Llano, I. (2005) Developmental changes in parvalbumin regulate presynaptic Ca^{2+} signaling. J. Neurosci. 25, 96–107

67 Freund, T. F. and Buzsaki, G. (1996) Interneurons of the hippocampus. Hippocampus 6, 347–470

68 Vreugdenhil, M., Jefferys, J. G., Celio, M. R. and Schwaller, B. (2003) Parvalbumin-deficiency facilitates repetitive IPSCs and gamma oscillations in the hippocampus. J. Neurophysiol. 89, 1414–1422

69 Muller, M., Felmy, F., Schwaller, B. and Schneggenburger, R. (2007) Parvalbumin is a mobile presynaptic Ca^{2+} buffer in the calyx of held that accelerates the decay of Ca^{2+} and short-term facilitation. J. Neurosci. 27, 2261–2271

70 Schmidt, H., Stiefel, K. M., Racay, P., Schwaller, B. and Eilers, J. (2003) Mutational analysis of dendritic Ca^{2+} kinetics in rodent Purkinje cells: Role of parvalbumin and calbindin D28k. J. Physiol. 551, 13–32

71 Mihaly, A., Szente, M., Dubravcsik, Z., Boda, B., Kiraly, E., Nagy, T. and Domonkos, A. (1997) Parvalbumin- and calbindin-containing neurons express c-fos protein in primary and secondary (mirror) epileptic foci of the rat neocortex. Brain Res. 761, 135–145

72 Schwaller, B., Tetko, I. V., Tandon, P., Silveira, D. C., Vreugdenhil, M., Henzi, T., Potier, M. C., Celio, M. R. and Villa, A. E. (2004) Parvalbumin deficiency affects network properties resulting in increased susceptibility to epileptic seizures. Mol. Cell. Neurosci. 25, 650–663

73 Cheron, G., Gall, D., Servais, L., Dan, B., Maex, R. and Schiffmann, S. N. (2004) Inactivation of calcium-binding protein genes induces 160 Hz oscillations in the cerebellar cortex of alert mice. J. Neurosci. 24, 434–441

74 Cheron, G., Servais, L., Dan, B., Gall, D., Roussel, C. and Schiffmann, S. N. (2005) Fast oscillation in the cerebellar cortex of calcium binding protein-deficient mice: A new sensorimotor arrest rhythm. Prog. Brain. Res. 148, 165–180

75 Farre-Castany, M. A., Schwaller, B., Gregory, P., Barski, J., Mariethoz, C., Eriksson, J. L., Tetko, I. V., Wolfer, D., Celio, M. R., Schmutz, I., Albrecht, U. and Villa, A. E. (2007) Differences in locomotor behavior revealed in mice deficient for the calcium-binding proteins parvalbumin, calbindin D-28k or both. Behav. Brain Res. 178, 250–261

76 Servais, L., Bearzatto, B., Schwaller, B., Dumont, M., De Saedeleer, C., Dan, B., Barski, J. J., Schiffmann, S. N. and Cheron, G. (2005) Mono- and dual-frequency fast cerebellar oscillation in mice lacking parvalbumin and/or calbindin D-28k. Eur. J. Neurosci. 22, 861–870

77 Andressen, C., Blümcke, I. and Celio, M. R. (1993) Calcium-binding proteins: Selective markers of nerve cells. Cell Tissue Res. 271, 181–208

78 Baimbridge, K. G., Celio, M. R. and Rogers, J. H. (1992) Calcium-binding proteins in the nervous system. Trends Neurosci. 15, 303–308

79 Schneeberger, P. R. and Heizmann, C. W. (1986) Parvalbumin in rat kidney. Purification and localization. FEBS Lett. 201, 51–56

80 Loffing, J., Loffing-Cueni, D., Valderrabano, V., Klausli, L., Hebert, S. C., Rossier, B. C., Hoenderop, J. G., Bindels, R. J. and Kaissling, B. (2001) Distribution of transcellular calcium and sodium transport pathways along mouse distal nephron. Am. J. Physiol. Renal. Physiol. 281, F1021–1027

81 Voets, T., Nilius, B., Hoefs, S., van der Kemp, A. W., Droogmans, G., Bindels, R. J. and Hoenderop, J. G. (2004) TRPM6 forms the Mg^{2+} influx channel involved in intestinal and renal Mg^{2+} absorption. J. Biol. Chem. 279, 19–25

82 Belge, H., Gailly, P., Schwaller, B., Loffing, J., Debaix, H., Riveira-Munoz, E., Beauwens, R., Devogelaer, J. P., Hoenderop, J. G., Bindels, R. J. and Devuyst, O. (2007) Renal expression of parvalbumin is critical for NaCl handling and response to diuretics. Proc. Natl. Acad. Sci. USA 104, 14849–14854

83 Glenmark, B., Nilsson, M., Gao, H., Gustafsson, J. A., Dahlman-Wright, K. and Westerblad, H. (2004) Difference in skeletal muscle function in males vs. females: Role of estrogen receptor-beta. Am. J. Physiol. Endocrinol. Metab. 287, E1125–1131

84 Blurton-Jones, M. and Tuszynski, M. H. (2002) Estrogen receptor-beta colocalizes extensively with parvalbumin-labeled inhibitory neurons in the cortex, amygdala, basal forebrain, and hippocampal formation of intact and ovariectomized adult rats. J. Comp. Neurol. 452, 276–287

85 Huber, B. and Pette, D. (1996) Dynamics of parvalbumin expression in low-frequency-stimulated fast- twitch rat muscle. Eur. J. Biochem. 236, 814–819

86 Leberer, E. and Pette, D. (1986) Neural regulation of parvalbumin expression in mammalian skeletal muscle. Biochem. J. 235, 67–73

87 Gabriel, R., Lesauter, J., Banvolgyi, T., Petrovics, G., Silver, R. and Witkovsky, P. (2004) AII amacrine neurons of the rat retina show diurnal and circadian rhythms of parvalbumin immunoreactivity. Cell Tissue Res. 315, 181–186

88 Devarajan, K., Marchant, E. G. and Rusak, B. (2005) Circadian and light regulation of oxytocin and parvalbumin protein levels in the ciliated ependymal layer of the third ventricle in the C57 mouse. Neuroscience 134, 539–547

89 Sakaguchi, N., Henzl, M. T., Thalmann, I., Thalmann, R. and Schulte, B. A. (1998) Oncomodulin is expressed exclusively by outer hair cells in the organ of Corti. J. Histochem. Cytochem. 46, 29–40
90 Yin, Y., Henzl, M. T., Lorber, B., Nakazawa, T., Thomas, T. T., Jiang, F., Langer, R. and Benowitz, L. I. (2006) Oncomodulin is a macrophage-derived signal for axon regeneration in retinal ganglion cells. Nat. Neurosci. 9, 843–852
91 Mutus, B., Karuppiah, N., Sharma, R. K. and MacManus, J. P. (1985) The differential stimulation of brain and heart cyclic-AMP phosphodiesterase by oncomodulin. Biochem. Biophys. Res. Commun. 131, 500–506
92 Hauk, T. G., Muller, A., Lee, J., Schwendener, R. and Fischer, D. (2008) Neuroprotective and axon growth promoting effects of intraocular inflammation do not depend on oncomodulin or the presence of large numbers of activated macrophages. Exp. Neurol. 209, 469–482
93 Brewer, J. M., Wunderlich, J. K., Kim, D. H., Carr, M. Y., Beach, G. G. and Ragland, W. L. (1989) Avian thymic hormone (ATH) is a parvalbumin. Biochem. Biophys. Res. Commun. 160, 1155–1161
94 Serda, R. E. and Henzl, M. T. (1991) Metal ion-binding properties of avian thymic hormone. J. Biol. Chem. 266, 7291–7299
95 Brewer, J. M., Arnold, J., Beach, G. G., Ragland, W. L. and Wunderlich, J. K. (1991) Comparison of the amino acid sequences of tissue-specific parvalbumins from chicken muscle and thymus and possible evolutionary significance. Biochem. Biophys. Res. Commun. 181, 226–231
96 Hapak, R. C., Zhao, H., Boschi, J. M. and Henzl, M. T. (1994) Novel avian thymic parvalbumin displays high degree of sequence homology to oncomodulin. J. Biol. Chem. 269, 5288–5296
97 Vasquez, G. M. and Ragland, W. L. (2005) Avian thymic hormone treatment of peripheral blood mononuclear cells from young chicks stimulates acute graft-*versus*-host reaction in chicken embryos. Dev. Comp. Immunol. 29, 663–668
98 Nelson, M. R., Thulin, E., Fagan, P. A., Forsen, S. and Chazin, W. J. (2002) The EF-hand domain: A globally cooperative structural unit. Protein Sci. 11, 198–205
99 Kordel, J., Forsen, S. and Chazin, W. J. (1989) 1H NMR sequential resonance assignments, secondary structure, and global fold in solution of the major (trans-Pro43) form of bovine calbindin D9k. Biochemistry 28, 7065–7074
100 Skelton, N. J., Forsen, S. and Chazin, W. J. (1990) ^{1}H NMR resonance assignments, secondary structure, and global fold of Apo bovine calbindin D9k. Biochemistry 29, 5752–5761
101 Chazin, W. and Veenstra, T. D. (1999) Determination of the metal-binding cooperativity of wild-type and mutant calbindin D9K by electrospray ionization mass spectrometry. Rapid Commun. Mass Spectrom. 13, 548–555
102 Kordel, J., Skelton, N. J., Akke, M. and Chazin, W. J. (1993) High-resolution structure of calcium-loaded calbindin D9k. J. Mol. Biol. 231, 711–734
103 Finn, B. E., Kordel, J., Thulin, E., Sellers, P. and Forsen, S. (1992) Dissection of calbindin D9k into two Ca^{2+}-binding subdomains by a combination of mutagenesis and chemical cleavage. FEBS Lett. 298, 211–214
104 Linse, S., Johansson, C., Brodin, P., Grundstrom, T., Drakenberg, T. and Forsen, S. (1991) Electrostatic contributions to the binding of Ca^{2+} in calbindin D9k. Biochemistry 30, 154–162
105 Andersson, M., Malmendal, A., Linse, S., Ivarsson, I., Forsen, S. and Svensson, L. A. (1997) Structural basis for the negative allostery between Ca^{2+}- and Mg^{2+}-binding in the intracellular Ca^{2+}-receptor calbindin D9k. Protein Sci. 6, 1139–1147
106 Skelton, N. J., Kördel, J., Akke, M., Forsén, S. and Chazin, W. J. (1994) Signal transduction versus buffering activity in Ca^{2+}-binding proteins. Nat. Struct. Biol. 1, 239–245
107 Bindels, R. J., Hartog, A., Timmermans, J. A. and van Os, C. H. (1991) Immunocytochemical localization of calbindin-D28k, calbindin-D9k and parvalbumin in rat kidney. Contrib. Nephrol. 91, 7–13
108 Schwaller, B., Durussel, I., Jermann, D., Herrmann, B. and Cox, J. A. (1997) Comparison of the Ca^{2+}-binding properties of human recombinant calretinin-22k and calretinin. J. Biol. Chem. 272, 29663–29671
109 Winsky, L. and Kuznicki, J. (1996) Antibody recognition of calcium-binding proteins depends on their calcium-binding status. J. Neurochem. 66, 1–8
110 Lee, G. S., Choi, K. C. and Jeung, E. B. (2006) Glucocorticoids differentially regulate expression of duodenal and renal calbindin-D9k through glucocorticoid receptor-mediated pathway in mouse model. Am. J. Physiol. Endocrinol. Metab. 290, E299–307
111 Huybers, S., Naber, T. H., Bindels, R. J. and Hoenderop, J. G. (2007) Prednisolone-induced Ca^{2+} malabsorption is caused by diminished expression of the epithelial Ca^{2+} channel TRPV6. Am. J. Physiol. Gastrointest. Liver Physiol. 292, G92–97
112 Choi, K. C. and Jeung, E. B. (2008) Molecular mechanism of regulation of the calcium-binding protein calbindin-D(9k), and its physiological role(s) in mammals: A review of current research. J. Cell. Mol. Med. 12, 409–420
113 Darwish, H., Krisinger, J., Furlow, J. D., Smith, C., Murdoch, F. E. and DeLuca, H. F. (1991) An estrogen-responsive element mediates the transcriptional regulation of calbindin D-9K gene in rat uterus. J. Biol. Chem. 266, 551–558
114 Fujimoto, N., Igarashi, K., Kanno, J., Honda, H. and Inoue, T. (2004) Identification of estrogen-responsive genes in the GH3 cell line by cDNA microarray analysis. J. Steroid Biochem. Mol. Biol. 91, 121–129
115 Dang, V. H., Choi, K. C., Hyun, S. H. and Jeung, E. B. (2007) Induction of uterine calbindin-D9k through an estrogen receptor-dependent pathway following single injection with xenobiotic agents in immature rats. J. Toxicol. Environ. Health A 70, 171–182
116 Lee, G. S., Choi, K. C., Han, H. J. and Jeung, E. B. (2007) The classical and a non-classical pathways associated with NF-kappaB are involved in estrogen-mediated regulation of calbindin-D9k gene in rat pituitary cells. Mol. Cell. Endocrinol. 277, 42–50
117 Cao, L. P., Bolt, M. J., Wei, M., Sitrin, M. D. and Chun Li, Y. (2002) Regulation of calbindin-D9k expression by 1,25-dihydroxyvitamin D(3) and parathyroid hormone in mouse primary renal tubular cells. Arch. Biochem. Biophys. 400, 118–124
118 Hemmingsen, C., Staun, M. and Olgaard, K. (1994) Effects of magnesium on renal and intestinal calbindin-D. Miner. Electrolyte Metab. 20, 265–273
119 Bindels, R. J., Timmermans, J. A., Hartog, A., Coers, W. and van Os, C. H. (1991) Calbindin-D9k and parvalbumin are exclusively located along basolateral membranes in rat distal nephron. J. Am. Soc. Nephrol. 2, 1122–1129
120 Feher, J. J., Fullmer, C. S. and Wasserman, R. H. (1992) Role of facilitated diffusion of calcium by calbindin in intestinal calcium absorption. Am. J. Physiol. 262, C517-C526
121 Fleet, J. C. and Wood, R. J. (1994) Identification of calbindin D-9k mRNA and its regulation by 1,25-dihydroxyvitamin D3 in CaCo-2 cells. Arch. Biochem. Biophys. 308, 171–174
122 Cheung, W. T., Richards, D. E. and Rogers, J. H. (1993) Calcium binding by chick calretinin and rat calbindin D28k synthesised in bacteria. Eur. J. Biochem. 215, 401–410
123 Akerfeldt, K. S., Coyne, A. N., Wilk, R. R., Thulin, E. and Linse, S. (1996) Ca^{2+}-binding stoichiometry of calbindin D28k as assessed by spectroscopic analyses of synthetic peptide fragments. Biochemistry 35, 3662–3669
124 Cedervall, T., Andre, I., Selah, C., Robblee, J. P., Krecioch, P. C., Fairman, R., Linse, S. and Akerfeldt, K. S. (2005) Calbindin D28k EF-hand ligand binding and oligomerization: Four high-affinity sites – three modes of action. Biochemistry 44, 13522–13532

125 Nagerl, U. V., Novo, D., Mody, I. and Vergara, J. L. (2000) Binding kinetics of calbindin-D(28k) determined by flash photolysis of caged Ca^{2+}. Biophys. J. 79, 3009–3018

126 Berggard, T., Miron, S., Onnerfjord, P., Thulin, E., Akerfeldt, K. S., Enghild, J. J., Akke, M. and Linse, S. (2002) Calbindin D28k exhibits properties characteristic of a Ca^{2+} sensor. J. Biol. Chem. 277, 16662–16672

127 Airaksinen, M. S., Eilers, J., Garaschuk, O., Thoenen, H., Konnerth, A. and Meyer, M. (1997) Ataxia and altered dendritic calcium signaling in mice carrying a targeted null mutation of the calbindin D28k gene. Proc. Natl. Acad. Sci. USA 94, 1488–1493

128 Schmidt, H., Schwaller, B. and Eilers, J. (2005) Calbindin D28k targets myo-inositol monophosphatase in spines and dendrites of cerebellar Purkinje neurons. Proc. Natl. Acad. Sci. USA 102, 5850–5855

129 Berggard, T., Szczepankiewicz, O., Thulin, E. and Linse, S. (2002) Myo-inositol monophosphatase is an activated target of calbindin D28k. J. Biol. Chem. 277, 41954–41959

130 Lutz, W., Frank, E. M., Craig, T. A., Thompson, R., Venters, R. A., Kojetin, D., Cavanagh, J. and Kumar, R. (2003) Calbindin D28K interacts with Ran-binding protein M: Identification of interacting domains by NMR spectroscopy. Biochem. Biophys. Res. Commun. 303, 1186–1192

131 Bellido, T., Huening, M., Raval-Pandya, M., Manolagas, S. C. and Christakos, S. (2000) Calbindin-D28k is expressed in osteoblastic cells and suppresses their apoptosis by inhibiting caspase-3 activity. J. Biol. Chem. 275, 26328–26332

132 Reisner, P. D., Christakos, S. and Vanaman, T. C. (1992) *In vitro* enzyme activation with calbindin-D28k, the vitamin D-dependent 28 kDa calcium binding protein. FEBS Lett. 297, 127–131

133 Morgan, D. W., Welton, A. F., Heick, A. E. and Christakos, S. (1986) Specific *in vitro* activation of Ca,Mg-ATPase by vitamin D-dependent rat renal calcium binding protein (calbindin D28K). Biochem. Biophys. Res. Commun. 138, 547–553

134 Christakos, S., Dhawan, P., Peng, X., Obukhov, A. G., Nowycky, M. C., Benn, B. S., Zhong, Y., Liu, Y. and Shen, Q. (2007) New insights into the function and regulation of vitamin D target proteins. J. Steroid Biochem. Mol. Biol. 103, 405–410

135 Lambers, T. T., Mahieu, F., Oancea, E., Hoofd, L., de Lange, F., Mensenkamp, A. R., Voets, T., Nilius, B., Clapham, D. E., Hoenderop, J. G. and Bindels, R. J. (2006) Calbindin-D28K dynamically controls TRPV5-mediated Ca^{2+} transport. EMBO J. 25, 2978–2988

136 Kojetin, D. J., Venters, R. A., Kordys, D. R., Thompson, R. J., Kumar, R. and Cavanagh, J. (2006) Structure, binding interface and hydrophobic transitions of Ca^{2+}-loaded calbindin-D(28K). Nat. Struct. Mol. Biol. 13, 641–647

137 Kim, J. H., Lee, J. A., Song, Y. M., Park, C. H., Hwang, S. J., Kim, Y. S., Kaang, B. K. and Son, H. (2006) Overexpression of calbindin-D28K in hippocampal progenitor cells increases neuronal differentiation and neurite outgrowth. FASEB J. 20, 109–111

138 Zhang, C., Sun, Y., Wang, W., Zhang, Y., Ma, M. and Lou, Z. (2008) Crystallization and preliminary crystallographic analysis of human Ca^{2+}-loaded calbindin-D28k. Acta Crystallogr. Sect. F Struct. Biol. Cryst. Commun. 64, 133–136

139 Sooy, K., Schermerhorn, T., Noda, M., Surana, M., Rhoten, W. B., Meyer, M., Fleischer, N., Sharp, G. W. and Christakos, S. (1999) Calbindin-D(28k) controls $[Ca^{2+}](i)$ and insulin release. Evidence obtained from calbindin-d(28k) knockout mice and beta cell lines. J. Biol. Chem. 274, 34343–34349

140 Reddy, D., Pollock, A. S., Clark, S. A., Sooy, K., Vasavada, R. C., Stewart, A. F., Honeyman, T. and Christakos, S. (1997) Transfection and overexpression of the calcium binding protein calbindin-D28k results in a stimulatory effect on insulin synthesis in a rat beta cell line (RIN 1046–38). Proc. Natl. Acad. Sci. USA 94, 1961–1966

141 Mattson, M. P., Rychlik, B., Chu, C. and Christakos, S. (1991) Evidence for calcium-reducing and excito-protective roles for the calcium-binding protein calbindin-D28k in cultured hippocampal neurons. Neuron 6, 41–51

142 Iacopino, A., Christakos, S., German, D., Sonsalla, P. K. and Altar, C. A. (1992) Calbindin-D28K-containing neurons in animal models of neurodegeneration: Possible protection from excitotoxicity. Brain Res. Mol. Brain Res. 13, 251–261

143 Airaksinen, M. S., Thoenen, H. and Meyer, M. (1997) Vulnerability of midbrain dopaminergic neurons in calbindin-D-28k-deficient mice: Lack of evidence for a neuroprotective role of endogenous calbindin in MPTP-treated and weaver mice. Eur. J. Neurosci. 9, 120–127

144 Phillips, R. G., Meier, T. J., Giuli, L. C., McLaughlin, J. R., Ho, D. Y. and Sapolsky, R. M. (1999) Calbindin D28K gene transfer *via* herpes simplex virus amplicon vector decreases hippocampal damage *in vivo* following neurotoxic insults. J. Neurochem. 73, 1200–1205

145 Yenari, M. A., Minami, M., Sun, G. H., Meier, T. J., Kunis, D. M., McLaughlin, J. R., Ho, D. Y., Sapolsky, R. M. and Steinberg, G. K. (2001) Calbindin d28k overexpression protects striatal neurons from transient focal cerebral ischemia. Stroke 32, 1028–1035

146 D'Orlando, C., Celio, M. R. and Schwaller, B. (2002) Calretinin and calbindin D-28k, but not parvalbumin protect against glutamate-induced excitotoxicity in transfected N18-RE 105 neuroblastoma-retina hybrid cells. Brain Res. 945, 181–190

147 Barski, J. J., Morl, K. and Meyer, M. (2002) Conditional inactivation of the calbindin D-28k (Calb1) gene by Cre/loxP-mediated recombination. Genesis 32, 165–168

148 Barski, J. J., Hartmann, J., Rose, C. R., Hoebeek, F., Morl, K., Noll-Hussong, M., De Zeeuw, C. I., Konnerth, A. and Meyer, M. (2003) Calbindin in cerebellar Purkinje cells is a critical determinant of the precision of motor coordination. J. Neurosci. 23, 3469–3477

149 Matsumoto, M., Nakagawa, T., Inoue, T., Nagata, E., Tanaka, K., Takano, H., Minowa, O., Kuno, J., Sakakibara, S., Yamada, M., Yoneshima, H., Miyawaki, A., Fukuuchi, Y., Furuichi, T., Okano, H., Mikoshiba, K. and Noda, T. (1996) Ataxia and epileptic seizures in mice lacking type 1 inositol 1,4,5- trisphosphate receptor. Nature 379, 168–171

150 Blatow, M., Caputi, A., Burnashev, N., Monyer, H. and Rozov, A. (2003) Ca^{2+} buffer saturation underlies paired pulse facilitation in calbindin-D28k-containing terminals. Neuron 38, 79–88

151 Maeda, H., Ellis-Davies, G. C., Ito, K., Miyashita, Y. and Kasai, H. (1999) Supralinear Ca^{2+} signaling by cooperative and mobile Ca^{2+} buffering in Purkinje neurons. Neuron 24, 989–1002

152 Rozov, A., Burnashev, N., Sakmann, B. and Neher, E. (2001) Transmitter release modulation by intracellular Ca^{2+} buffers in facilitating and depressing nerve terminals of pyramidal cells in layer 2/3 of the rat neocortex indicates a target cell-specific difference in presynaptic calcium dynamics. J. Physiol. 531, 807–826

153 Zucker, R. S. and Regehr, W. G. (2002) Short-term synaptic plasticity. Annu. Rev. Physiol. 64, 355–405

154 Nagerl, U. V. and Mody, I. (1998) Calcium-dependent inactivation of high-threshold calcium currents in human dentate gyrus granule cells. J. Physiol. 509, 39–45

155 Klapstein, G. J., Vietla, S., Lieberman, D. N., Gray, P. A., Airaksinen, M. S., Thoenen, H., Meyer, M. and Mody, I. (1998) Calbindin-D28k fails to protect hippocampal neurons against ischemia in spite of its cytoplasmic calcium buffering properties: Evidence from calbindin-D28k knockout mice. Neuroscience 85, 361–373

156 Schmidt, H., Kunerth, S., Wilms, C., Strotmann, R. and Eilers, J. (2007) Spino-dendritic cross-talk in rodent Purkinje neurons mediated by endogenous Ca^{2+}-binding proteins. J. Physiol. 581, 619–629

157 Airaksinen, L., Virkkala, J., Aarnisalo, A., Meyer, M., Ylikoski, J. and Airaksinen, M. S. (2000) Lack of calbindin-D28k does not affect hearing level or survival of hair cells in acoustic trauma. ORL J. Otorhinolaryngol. Relat. Spec. 62, 9–12
158 Wassle, H., Peichl, L., Airaksinen, M. S. and Meyer, M. (1998) Calcium-binding proteins in the retina of a calbindin-null mutant mouse. Cell Tissue Res. 292, 211–218
159 Berridge, M. J., Bootman, M. D. and Roderick, H. L. (2003) Calcium signalling: Dynamics, homeostasis and remodelling. Nat. Rev. Mol. Cell. Biol. 4, 517–529
160 Hoenderop, J. G., van der Kemp, A. W., Hartog, A., van de Graaf, S. F., van Os, C. H., Willems, P. H. and Bindels, R. J. (1999) Molecular identification of the apical Ca^{2+} channel in 1, 25-dihydroxyvitamin D3-responsive epithelia. J. Biol. Chem. 274, 8375–8378
161 Zheng, W., Xie, Y., Li, G., Kong, J., Feng, J. Q. and Li, Y. C. (2004) Critical role of calbindin-D28k in calcium homeostasis revealed by mice lacking both vitamin D receptor and calbindin-D28k. J. Biol. Chem. 279, 52406–52413
162 Gkika, D., Hsu, Y. J., van der Kemp, A. W., Christakos, S., Bindels, R. J. and Hoenderop, J. G. (2006) Critical role of the epithelial Ca^{2+} channel TRPV5 in active Ca^{2+} reabsorption as revealed by TRPV5/calbindin-D28K knockout mice. J. Am. Soc. Nephrol. 17, 3020–3027
163 Nagerl, U. V., Mody, I., Jeub, M., Lie, A. A., Elger, C. E. and Beck, H. (2000) Surviving granule cells of the sclerotic human hippocampus have reduced Ca^{2+} influx because of a loss of calbindin-D(28k) in temporal lobe epilepsy. J. Neurosci. 20, 1831–1836
164 Kutuzova, G. D., Akhter, S., Christakos, S., Vanhooke, J., Kimmel-Jehan, C. and Deluca, H. F. (2006) Calbindin D(9k) knockout mice are indistinguishable from wild-type mice in phenotype and serum calcium level. Proc. Natl. Acad. Sci. USA 103, 12377–12381
165 Akhter, S., Kutuzova, G. D., Christakos, S. and DeLuca, H. F. (2007) Calbindin D9k is not required for 1,25-dihydroxyvitamin D3-mediated Ca^{2+} absorption in small intestine. Arch. Biochem. Biophys. 460, 227–232
166 Lee, G. S., Lee, K. Y., Choi, K. C., Ryu, Y. H., Paik, S. G., Oh, G. T. and Jeung, E. B. (2007) Phenotype of a calbindin-D9k gene knockout is compensated for by the induction of other calcium transporter genes in a mouse model. J. Bone Miner. Res. 22, 1968–1978
167 Benn, B. S., Ajibade, D., Porta, A., Dhawan, P., Hediger, M., Peng, J. B., Jiang, Y., Oh, G. T., Jeung, E. B., Lieben, L., Bouillon, R., Carmeliet, G. and Christakos, S. (2008) Active intestinal calcium transport in the absence of transient receptor potential vanilloid type 6 and calbindin-d9k. Endocrinology 149, 3196–3205
168 Hoenderop, J. G., Dardenne, O., Van Abel, M., Van Der Kemp, A. W., Van Os, C. H., St-Arnaud, R. and Bindels, R. J. (2002) Modulation of renal Ca^{2+} transport protein genes by dietary Ca^{2+} and 1,25-dihydroxyvitamin D3 in 25-hydroxyvitamin D3–1alpha-hydroxylase knockout mice. FASEB J. 16, 1398–1406
169 Huybers, S., Apostolaki, M., van der Eerden, B. C., Kollias, G., Naber, T. H., Bindels, R. J. and Hoenderop, J. G. (2008) Murine TNF(DeltaARE) Crohn's disease model displays diminished expression of intestinal Ca^{2+} transporters. Inflamm. Bowel Dis. 14, 803–811
170 Schwaller, B. (1996) Calretinin. In: Guidebook to the Calcium-Binding Proteins, pp. 26–28. Celio, M., Pauls, T. and Schwaller, B. (eds.), Oxford University Press, Oxford
171 Stevens, J. and Rogers, J. H. (1997) Chick calretinin: Purification, composition, and metal binding activity of native and recombinant forms. Protein Expr. Purif. 9, 171–181
172 Palczewska, M., Groves, P., Ambrus, A., Kaleta, A., Kover, K. E., Batta, G. and Kuznicki, J. (2001) Structural and biochemical characterization of neuronal calretinin domain I-II (residues 1–100). Comparison to homologous calbindin D28k domain I-II (residues 1–93). Eur. J. Biochem. 268, 6229–6237
173 Billing-Marczak, K. and Kuznicki, J. (1999) Calretinin-sensor or buffer function still unclear. Pol. J. Pharmacol. 51, 173–178
174 Faas, G. C., Schwaller, B., Vergara, J. L. and Mody, I. (2007) Resolving the fast kinetics of cooperative binding: Ca^{2+} buffering by calretinin. PLoS Biol. 5, e311
175 Faas, G. C., Karacs, K., Vergara, J. L. and Mody, I. (2005) Kinetic properties of DM-nitrophen binding to calcium and magnesium. Biophys. J. 88, 4421–4433
176 Freund, T. F. and Magloczky, Z. (1993) Early degeneration of calretinin-containing neurons in the rat hippocampus after ischemia. Neuroscience 56, 581–596
177 Hof, P. R., Glezer, I. I., Conde, F., Flagg, R. A., Rubin, M. B., Nimchinsky, E. A. and Vogt Weisenhorn, D. M. (1999) Cellular distribution of the calcium-binding proteins parvalbumin, calbindin, and calretinin in the neocortex of mammals: Phylogenetic and developmental patterns. J. Chem. Neuroanat. 16, 77–116
178 Lukas, W. and Jones, K. A. (1994) Cortical neurons containing calretinin are selectively resistant to calcium overload and excitotoxicity. Neuroscience 61, 307–316
179 Pike, C. J. and Cotman, C. W. (1995) Calretinin-immunoreactivity neurons are resistant to β-amyloid toxicity *in vitro.* Brain Res. 671, 293–298
180 Gander, J. C., Gotzos, V., Fellay, B. and Schwaller, B. (1996) Inhibition of the proliferative cycle and apoptotic events in WiDr cells after down-regulation of the calcium-binding protein calretinin using antisense oligodeoxynucleotides. Exp. Cell Res. 225, 399–410
181 Kuznicki, J., Isaacs, K. R. and Jacobowitz, D. M. (1996) The expression of calretinin in transfected PC12 cells provides no protection against Ca^{2+}-overload or trophic factor deprivation. Biochim. Biophys. Acta. 1313, 194–200
182 Billing-Marczak, K., Przybyszewska, M. and Kuznicki, J. (1999) Measurements of $[Ca^{2+}]$ using fura-2 in glioma C6 cells expressing calretinin with GFP as a marker of transfection: No Ca^{2+}-buffering provided by calretinin. Biochim. Biophys. Acta 1449, 169–177
183 Gall, D., Roussel, C., Susa, I., D'Angelo, E., Rossi, P., Bearzatto, B., Galas, M. C., Blum, D., Schurmans, S. and Schiffmann, S. N. (2003) Altered neuronal excitability in cerebellar granule cells of mice lacking calretinin. J. Neurosci. 23, 9320–9327
184 Schurmans, S., Schiffmann, S. N., Gurden, H., Lemaire, M., Lipp, H.-P., Schwam, V., Pochet, R., Imperato, A., Böhme, G. A. and Parmentier, M. (1997) Impaired LTP induction in the dentate gyrus of calretinin-deficient mice. Proc. Natl. Acad. Sci. USA 94, 10415–10420
185 Gurden, H., Schiffmann, S. N., Lemaire, M., Bohme, G. A., Parmentier, M. and Schurmans, S. (1998) Calretinin expression as a critical component in the control of dentate gyrus long-term potentiation induction in mice. Eur. J. Neurosci. 10, 3029–3033
186 Schiffmann, S. N., Cheron, G., Lohof, A., d'Alcantara, P., Meyer, M., Parmentier, M. and Schurmans, S. (1999) Impaired motor coordination and Purkinje cell excitability in mice lacking calretinin. Proc. Natl. Acad. Sci. USA 96, 5257–5262
187 de Solages, C., Szapiro, G., Brunel, N., Hakim, V., Isope, P., Buisseret, P., Rousseau, C., Barbour, B. and Lena, C. (2008) High-frequency organization and synchrony of activity in the purkinje cell layer of the cerebellum. Neuron 58, 775–788
188 Bearzatto, B., Servais, L., Roussel, C., Gall, D., Baba-Aissa, F., Schurmans, S., de Kerchove d'Exaerde, A., Cheron, G. and Schiffmann, S. N. (2006) Targeted calretinin expression in granule cells of calretinin-null mice restores normal cerebellar functions. FASEB J. 20, 380–382
189 Aller, M. I., Jones, A., Merlo, D., Paterlini, M., Meyer, A. H., Amtmann, U., Brickley, S., Jolin, H. E., McKenzie, A. N., Monyer, H., Farrant, M. and Wisden, W. (2003) Cerebellar granule cell Cre recombinase expression. Genesis 36, 97–103

190 John, L. M., Mosquera-Caro, M., Camacho, P. and Lechleiter, J. D. (2001) Control of IP(3)-mediated Ca^{2+} puffs in *Xenopus laevis* oocytes by the Ca^{2+}-binding protein parvalbumin. J. Physiol. 535, 3–16

191 Dargan, S. L. and Parker, I. (2003) Buffer kinetics shape the spatiotemporal patterns of IP3-evoked Ca^{2+} signals. J. Physiol. 553, 775–788

192 Edmonds, B., Reyes, R., Schwaller, B. and Roberts, W. M. (2000) Calretinin modifies presynaptic calcium signaling in frog saccular hair cells. Nat. Neurosci. 3, 786–790

193 Zhou, Z. and Neher, E. (1993) Mobile and immobile calcium buffers in bovine adrenal chromaffin cells. J. Physiol. 469, 245–273

194 Nowycky, M. C. and Pinter, M. J. (1993) Time courses of calcium and calcium-bound buffers following calcium influx in a model cell. Biophys. J. 64, 77–91

195 Sala, F. and Hernandez-Cruz, A. (1990) Calcium diffusion modeling in a spherical neuron. Relevance of buffering properties. Biophys. J. 57, 313–324

196 Möckel, V. and Fischer, G. (1994) Vulnerability to excitotoxic stimuli of cultured rat hippocampal neurons containing the calcium-binding proteins calretinin and calbindin D28k. Brain Res. 648, 109–120

197 Montpied, P., Winsky, L., Dailey, J. W., Jobe, P. C. and Jacobowitz, D. M. (1995) Alteration in levels of expression of brain calbindin D-28K and calretinin mRNA in genetically epilepsy-prone rats. Epilepsia 36, 911–921

198 Cargnello, R., Celio, M. R., Schwaller, B. and Gotzos, V. (1996) Change of calretinin expression in the human colon adenocarcinoma cell line HT29 after differentiation. Biochim. Biophys. Acta 1313, 201–208

199 Vogt Weisenhorn, D. M., Weruaga-Prieto, E. and Celio, M. R. (1996) Calretinin-immunoreactivity in organotypic cultures of the rat cerebral cortex: Effects of serum deprivation. Exp. Brain Res. 108, 101–112

200 Schwaller, B. and Herrmann, B. (1997) Regulated redistribution of calretinins in WiDr cells. Cell Death Differ. 4, 325–333

201 D'Orlando, C., Fellay, B., Schwaller, B., Salicio, V., Bloc, A., Gotzos, V. and Celio, M. R. (2001) Calretinin and calbindin D-28k delay the onset of cell death after excitotoxic stimulation in transfected P19 cells. Brain Res. 909, 145–158

202 Strauss, K. I., Kuznicki, J., Winsky, L., Kawagoe, J. I., Hammer, M. and Jacobowitz, D. M. (1997) The mouse calretinin gene promoter region: Structural and functional components. Brain Res. Mol. Brain Res. 49, 175–187

203 Billing-Marczak, K., Buzanska, L., Winsky, L., Nowotny, M., Rudka, T., Isaacs, K., Belin, M. F. and Kuznicki, J. (2002) AP2-like cis element is required for calretinin gene promoter activity in cells of neuronal phenotype differentiated from multipotent human cell line DEV. Biochim. Biophys. Acta 1577, 412–420

204 Billing-Marczak, K., Zieminska, E., Lesniak, W., Lazarewicz, J. W. and Kuznicki, J. (2004) Calretinin gene promoter activity is differently regulated in neurons and cancer cells. Role of AP2-like cis element and zinc ions. Biochim. Biophys. Acta 1678, 14–21

205 Schwaller, B., Celio, M. R. and Hunziker, W. (1995) Alternative splicing of calretinin mRNA leads to different forms of calretinin. Eur. J. Biochem. 230, 424–430

206 Schwaller, B., Meyer-Monard, S., Gander, J.-C., Pugin, P., Celio, M. R. and Ludwig, C. (1998) The calcium-binding protein calretinin-22k is detectable in the serum and specific cells of cancer patients. Anticancer Res. 18, 3361–3367

207 Schwaller, B., Celio, M. R. and Doglioni, C. (2004) Identification of calretinin and the alternatively spliced form calretinin-22k in primary pleural mesotheliomas and in their metastases. Anticancer Res. 24, 4003–4009

208 Gotzos, V., Vogt, P. and Celio, M. R. (1996) The calcium binding protein calretinin is a selective marker for malignant pleural mesotheliomas of the epithelial type. Pathol. Res. Pract. 192, 137–147

209 Doglioni, C., Tos, A. P. D., Laurino, L., Iuzzolino, P., Chiarelli, C., Celio, M. R. and Viale, G. (1996) Calretinin: A novel immunocytochemical marker for mesothelioma. Am. J. Surg. Pathol. 20, 1037–1046

210 Hack, N. J., Wride, M. C., Charters, K. M., Kater, S. B. and Parks, T. N. (2000) Developmental changes in the subcellular localization of calretinin. J. Neurosci. 20, RC67

211 Lasorsa, F. M., Pinton, P., Palmieri, L., Scarcia, P., Rottensteiner, H., Rizzuto, R. and Palmieri, F. (2008) Peroxisomes as novel players in cell calcium homeostasis. J. Biol. Chem. 283, 15300–15308

212 Carafoli, E., Genazzani, A. and Guerini, D. (1999) Calcium controls the transcription of its own transporters and channels in developing neurons. Biochem. Biophys. Res. Commun. 266, 624–632

213 Vecellio, M., Schwaller, B., Meyer, M., Hunziker, W. and Celio, M. R. (2000) Alterations in Purkinje cell spines of calbindin D-28 k and parvalbumin knock-out mice. Eur. J. Neurosci. 12, 945–954

214 Murchison, D. and Griffith, W. H. (2000) Mitochondria buffer non-toxic calcium loads and release calcium through the mitochondrial permeability transition pore and sodium/calcium exchanger in rat basal forebrain neurons. Brain Res. 854, 139–151

215 Chen, G., Racay, P., Bichet, S., Celio, M. R., Eggli, P. and Schwaller, B. (2006) Deficiency in parvalbumin, but not in calbindin D-28k upregulates mitochondrial volume and decreases smooth endoplasmic reticulum surface selectively in a peripheral, subplasmalemmal region in the soma of Purkinje cells. Neuroscience 142, 97–105

216 Chen, G., Carroll, S., Racay, P., Dick, J., Pette, D., Traub, I., Vrbova, G., Eggli, P., Celio, M. and Schwaller, B. (2001) Deficiency in parvalbumin increases fatigue resistance in fast-twitch muscle and upregulates mitochondria. Am. J. Physiol. 281, C114-C122

217 Maetzler, W., Nitsch, C., Bendfeldt, K., Racay, P., Vollenweider, F. and Schwaller, B. (2004) Ectopic parvalbumin expression in mouse forebrain neurons increases excitotoxic injury provoked by ibotenic acid injection into the striatum. Exp. Neurol. 186, 78–88

218 Van Den Bosch, L., Schwaller, B., Vleminckx, V., Meijers, B., Stork, S., Ruehlicke, T., Van Houtte, E., Klaassen, H., Celio, M. R., Missiaen, L., Robberecht, W. and Berchtold, M. W. (2002) Protective effect of parvalbumin on excitotoxic motor neuron death. Exp. Neurol. 174, 150–161

219 Dove, L. S., Nahm, S. S., Murchison, D., Abbott, L. C. and Griffith, W. H. (2000) Altered calcium homeostasis in cerebellar Purkinje cells of leaner mutant mice. J. Neurophysiol. 84, 513–524

220 Murchison, D., Dove, L. S., Abbott, L. C. and Griffith, W. H. (2002) Homeostatic compensation maintains Ca^{2+} signaling functions in Purkinje neurons in the leaner mutant mouse. Cerebellum 1, 119–127

221 Murchison, D. and Griffith, W. H. (2007) Calcium buffering systems and calcium signaling in aged rat basal forebrain neurons. Aging Cell 6, 297–305

222 Zühlke, R. D., Pitt, G. S., Deisseroth, K., Tsien, R. W. and Reuter, H. (1999) Calmodulin supports both inactivation and facilitation of L-type calcium channels. Nature 399, 159–162

223 Lee, A., Wong, S. T., Gallagher, D., Li, B., Storm, D. R., Scheuer, T. and Catterall, W. A. (1999) Ca^{2+}/calmodulin binds to and modulates P/Q-type calcium channels. Nature 399, 155–159

224 Kreiner, L. and Lee, A. (2005) Endogenous and exogenous Ca^{2+} buffers differentially modulate Ca^{2+}-dependent inactivation of CAV2.1 Ca^{2+} channels. J. Biol. Chem. 281, 4691–4698

225 Ueno, T., Kameyama, K., Hirata, M., Ogawa, M., Hatsuse, H., Takagaki, Y., Ohmura, M., Osawa, N. and Kudo, Y. (2002) A mouse with a point mutation in plasma membrane Ca^{2+}-ATPase isoform 2 gene showed the reduced Ca^{2+} influx in cerebellar neurons. Neurosci. Res. 42, 287–297

226 Kurnellas, M. P., Lee, A. K., Li, H., Deng, L., Ehrlich, D. J. and Elkabes, S. (2007) Molecular alterations in the cerebellum of the plasma membrane calcium ATPase 2 (PMCA2)-null mouse indicate abnormalities in Purkinje neurons. Mol. Cell. Neurosci. 34, 178–188
227 Marsden, B. J., Shaw, G. S. and Sykes, B. D. (1990) Calcium binding proteins. Elucidating the contributions to calcium affinity from an analysis of species variants and peptide fragments. Biochem. Cell Biol. 68, 587–601
228 Moreland, J. L., Gramada, A., Buzko, O. V., Zhang, Q. and Bourne, P. E. (2005) The Molecular Biology Toolkit (MBT): A modular platform for developing molecular visualization applications. BMC Bioinformatics 6, 21
229 Markram, H., Roth, A. and Helmchen, F. (1998) Competitive calcium binding: Implications for dendritic calcium signaling. J. Comput. Neurosci. 5, 331–348
230 Bouilleret, V., Schwaller, B., Schurmans, S., Celio, M. R. and Fritschy, J. M. (2000) Neurodegenerative and morphogenic changes in a mouse model of temporal lobe epilepsy do not depend on the expression of the calcium-binding proteins parvalbumin, calbindin, or calretinin. Neuroscience 97, 47–58
231 Beers, D. R., Ho, B. K., Siklos, L., Alexianu, M. E., Mosier, D. R., Mohamed, A. H., Otsuka, Y., Kozovska, M. E., McAlhany, R. E., Smith, R. G. and Appel, S. H. (2001) Parvalbumin overexpression alters immune-mediated increases in intracellular calcium, and delays disease onset in a transgenic model of familial amyotrophic lateral sclerosis. J. Neurochem. 79, 499–509
232 Meyer, A. H., Katona, I., Blatow, M., Rozov, A. and Monyer, H. (2002) In vivo labeling of parvalbumin-positive interneurons and analysis of electrical coupling in identified neurons. J. Neurosci. 22, 7055–7064
233 Eberhard, M. and Erne, P. (1994) Calcium and magnesium binding to rat parvalbumin. Eur. J. Biochem. 222, 21–26
234 Martin, S. R., Linse, S., Johansson, C., Bayley, P. M. and Forsen, S. (1990) Protein surface charges and Ca^{2+} binding to individual sites in calbindin D9k: Stopped-flow studies. Biochemistry 29, 4188–4193
235 Naraghi, M. (1997) T-jump study of calcium binding kinetics of calcium chelators. Cell Calcium 22, 255–268
236 Permiakov, E. A., Ostrovskii, A., V., Kalinichenko, L. P. and Deikus, G. I. (1987) Kinetics of dissociation of parvalbumin complexes with calcium and magnesium ions. Mol. Biol. (Mosk) 21, 1017–1022
237 Akke, M., Forsen, S. and Chazin, W. J. (1991) Molecular basis for co-operativity in Ca^{2+} binding to calbindin D9k. 1H nuclear magnetic resonance studies of (Cd^{2+})1-bovine calbindin D9k. J. Mol. Biol. 220, 173–189
238 Allbritton, N. L., Meyer, T. and Stryer, L. (1992) Range of messenger action of calcium ion and inositol 1,4,5,-trisphophate. Science 258, 1812–1815
239 Gabso, M., Neher, E. and Spira, M. E. (1997) Low mobility of the Ca^{2+} buffers in axons of cultured Aplysia neurons. Neuron 18, 473–481
240 Gifford, J. L., Walsh, M. P. and Vogel, H. J. (2007) Structures and metal-ion-binding properties of the Ca^{2+}-binding helix-loop-helix EF-hand motifs. Biochem. J. 2007 405, 199–221